



School on QCD, Copanello, Italy

July 2007

**“High Energy Limit of QCD:
BFKL Cross Sections”**

1. Introduction to Small x Physics
2. Iterative view of the BFKL equation
3. Short range correlations
4. A look at renormalization-group improved equation
5. Azimuthal angles in Mueller–Navelet jets

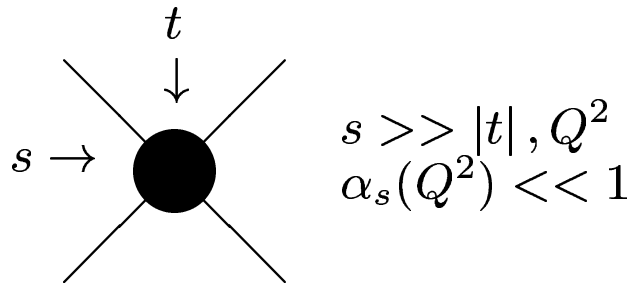
Agustín Sabio Vera
CERN



1. Introduction to Small x Physics

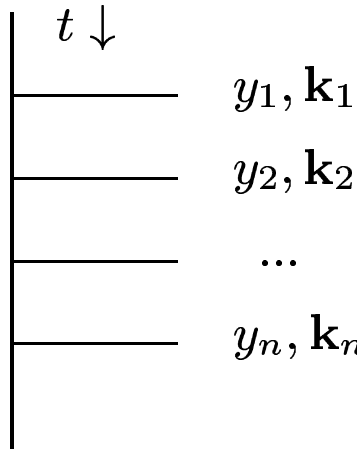


High energy limit of scattering amplitudes in perturbative QCD:



Large logarithms in s compensate small α_s : $\alpha_s \ln s \sim 1$

All orders resummation in multi-Regge kinematics: LL BFKL (70's)

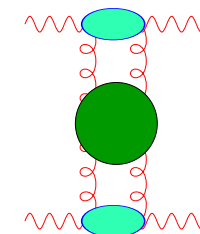


$$Y \sim \ln s$$

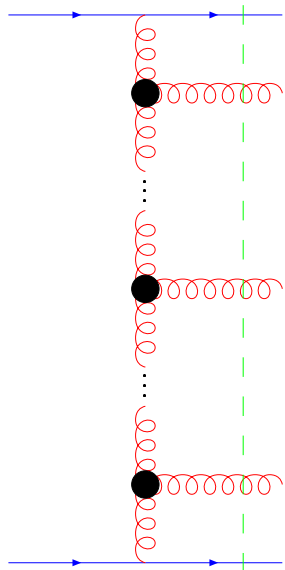
$$\mathbf{k}_i \sim \mathbf{k}_{i+1}$$

$$y_i \ll y_{i+1}$$

$$\alpha_s^n \int_0^Y dy_1 \int_0^{y_1} dy_2 \dots \int_0^{y_{n-1}} dy_n \sim \frac{(\alpha_s Y)^n}{n!}$$



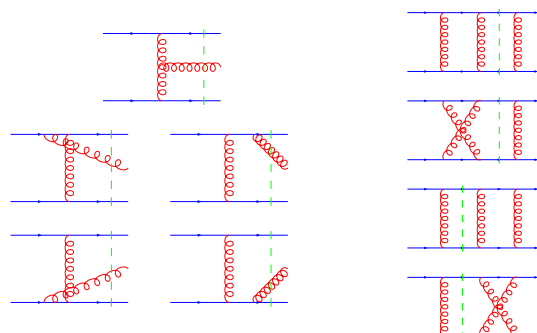
New Effective degrees of freedom:



Reggeized gluons in the t -channel

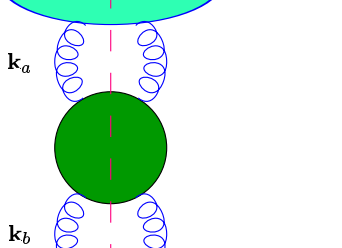
$$D_{\mu\nu}(s, q^2) = -i \frac{g_{\mu\nu}}{q^2} \left(\frac{s}{s_0}\right)^{\omega(q^2)} \rightarrow \text{Gluon Trajectory}$$

Effective Vertex for s -channel real emission



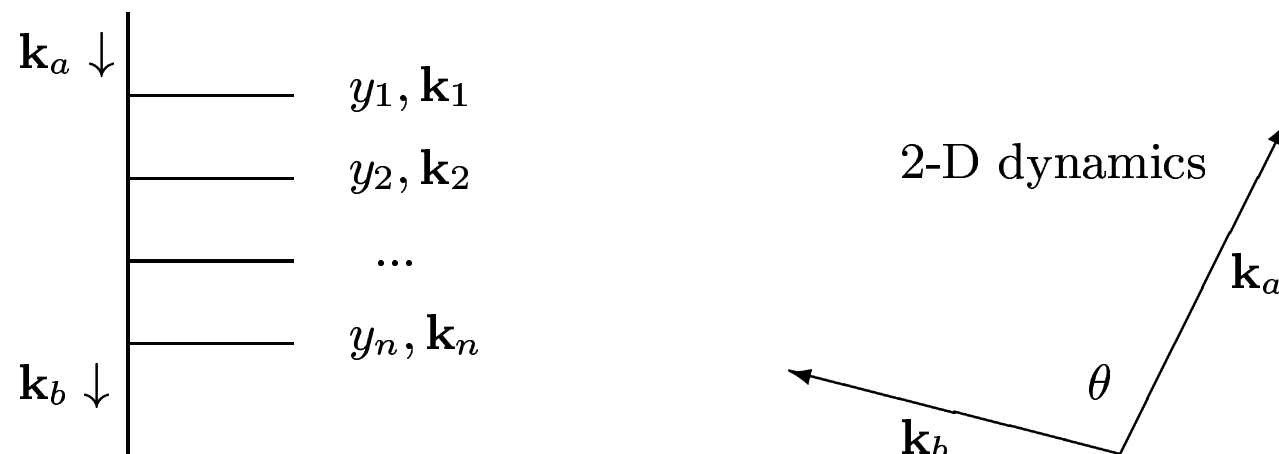
1. Introduction to Small x Physics

$$A \rightarrow \text{Oval} \rightarrow \sigma(s) = \int \frac{d^2 \mathbf{k}_a}{\mathbf{k}_a^2} \int \frac{d^2 \mathbf{k}_b}{\mathbf{k}_b^2} \Phi_A(\mathbf{k}_a) \Phi_B(\mathbf{k}_b) \mathcal{f} \left(\mathbf{k}_a, \mathbf{k}_b, Y = \ln \frac{s}{s_0} \right)$$



$$\mathcal{f}(\mathbf{k}_a, \mathbf{k}_b, Y) = \frac{1}{2\pi i} \int_{a-i\infty}^{a+i\infty} d\omega e^{\omega Y} f_\omega(\mathbf{k}_a, \mathbf{k}_b)$$

$$B \rightarrow \text{Oval} \rightarrow \omega f_\omega(\mathbf{k}_a, \mathbf{k}_b) = \delta^{(2)}(\mathbf{k}_a - \mathbf{k}_b) + \int d^2 \mathbf{k} \mathcal{K}(\mathbf{k}_a, \mathbf{k}) f_\omega(\mathbf{k}, \mathbf{k}_b)$$

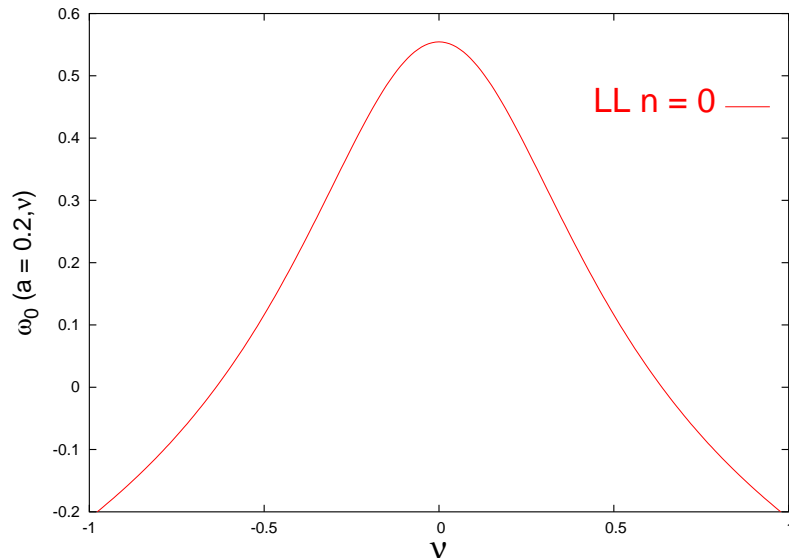


1. Introduction to Small x Physics

$$f(\mathbf{k}_a, \mathbf{k}_b, Y) \sim \sum_{n=-\infty}^{\infty} \int \frac{d\omega}{2\pi i} e^{\omega Y} \int \frac{d\gamma}{2\pi i} \left(\frac{\mathbf{k}_a^2}{\mathbf{k}_b^2} \right)^{\gamma - \frac{1}{2}} \frac{e^{in\theta}}{\omega - \omega_n(\bar{\alpha}_s, \gamma)}$$

$$\omega_n = \int d^2 \vec{q} \mathcal{K}(\vec{k}, \vec{q}) \left(\frac{\vec{q}^2}{\vec{k}^2} \right)^{\gamma - 1} e^{in\theta} =$$

$$\bar{\alpha}_s \left(2\Psi(1) - \Psi\left(\gamma + \frac{|n|}{2}\right) - \Psi\left(1 - \gamma + \frac{|n|}{2}\right) \right)$$



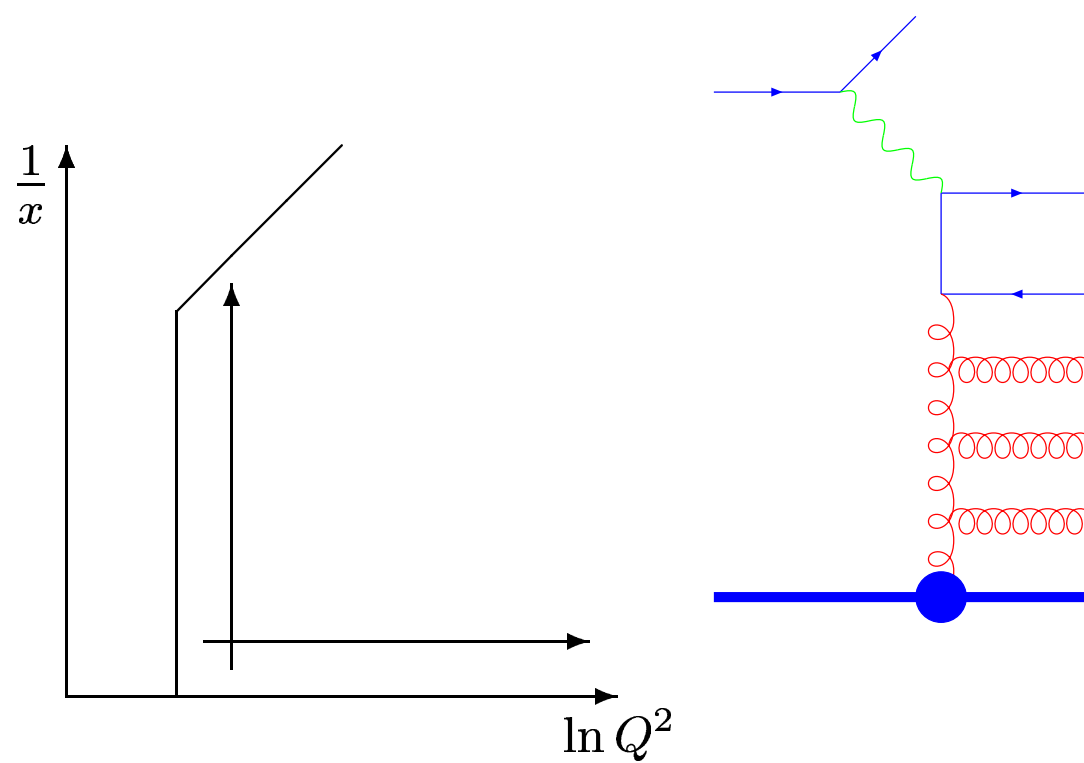
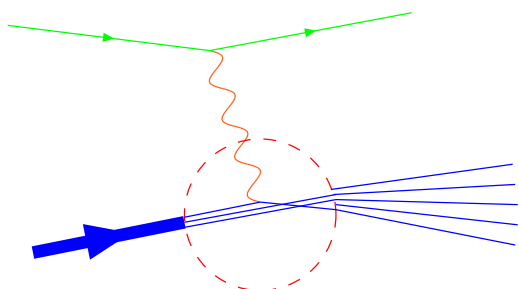
$n = 0$ dominates Cross Sections: Saddle point @ $\gamma = \frac{1}{2} + i\nu \dots$

Large s behaviour: $\boxed{\sigma \sim s^\lambda}$ $\lambda = \frac{\alpha_s N_c}{\pi} 4 \ln 2 \sim 0.5$ for $\alpha_s = 0.2$.

HARD or LL BFKL POMERON intercept

1. Introduction to Small x Physics

Why Small x Physics?: Connexion to DIS and evolution equations: $x \sim \frac{Q^2}{s}$



Singlet BFKL (Hard Pomeron): A bound state of two Reggeized gluons:

$$2 \frac{\partial f(\mathbf{q}, \mathbf{k}, y)}{\partial(\bar{\alpha}_s y)} = \int \frac{d^2 \mathbf{k}'}{\pi} \left(\frac{\mathbf{k}'^2 (\mathbf{k} - \mathbf{q})^2 + \mathbf{k}^2 (\mathbf{k}' - \mathbf{q})^2 - \mathbf{q}^2 (\mathbf{k} - \mathbf{k}')^2}{(\mathbf{k} - \mathbf{k}')^2 \mathbf{k}^2 (\mathbf{k} - \mathbf{q})^2} \right) f(\mathbf{q}, \mathbf{k}', y) \\ - [\ln(\mathbf{k}^2) - \ln((\mathbf{k} - \mathbf{q})^2)] f(\mathbf{q}, \mathbf{k}, y)$$

Express momenta in complex plane: $q = q_x + iq_y$, $q^* + q_x - iq_y$:

$$2 \frac{\partial f(q, q^*, k, k^*, y)}{\partial(\bar{\alpha}_s y)} = \int \frac{dk' dk'^*}{\pi} \left(\frac{(kk'^*(k - q)^*(k' - q) + h.c.)}{|(k - k')|^2 |k|^2 |(k - q)|^2} \right) f(q, q^*, k', k'^*, y) \\ - [\ln(|k|^2) - \ln(|(k - q)|^2)] f(q, q^*, k, k^*, y)$$

Fourier transform into impact parameters z_1 and z_2

$$\tilde{f}(z_1, z_1^*, z_2, z_2^*, y) = \int \frac{dk dk^* dq dq^*}{(2\pi)^4} e^{i(k^* \frac{(z_1 - z_2)}{2} + h.c.)} e^{i(q^* \frac{z_2}{2} + h.c.)} f(q, q^*, k, k^*, y)$$

1. Introduction to Small x Physics

Schrödinger-like equation: $\frac{\partial \tilde{f}(z_1, z_1^*, z_2, z_2^*, y)}{\partial y} = \tilde{H}_{1,2} \tilde{f}(z_1, z_1^*, z_2, z_2^*, y)$

Holomorphic separability: $\tilde{H}_{1,2} = H_{1,2} + \bar{H}_{1,2}$ with

$$H_{1,2} = -\frac{\bar{\alpha}}{2} \left(\ln(\partial_{z_1}) + (\partial_{z_1})^{-1} \ln(z_1 - z_2) \partial_{z_1} + z_1 \leftrightarrow z_2 - 2\Psi(1) \right)$$

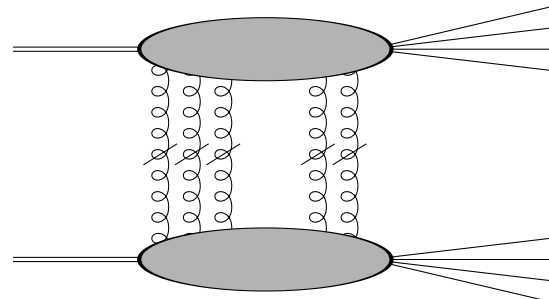
$\tilde{\phi}(z_1, z_1^*, z_2, z_2^*, y) = \chi(z_1, z_2, y) \bar{\chi}(z_1^*, z_2^*, y)$, with $\chi, \bar{\chi}$ eigenfunctions of H, \bar{H} .

$s = 0$ Möbius invariance of H, \bar{H} (translation and inversion)

$$H'_{1,2} = -\frac{\bar{\alpha}}{2} \left(\ln(z_1^2 \partial_{z_1}) + (\partial_{z_1})^{-1} \ln \left(\frac{(z_1 - z_2)}{z_1 z_2} \right) \partial_{z_1} + z_1 \leftrightarrow z_2 - 2\Psi(1) \right)$$

$H_{1,2} = -\frac{\bar{\alpha}}{2} (\Psi(1 + J) + \Psi(-J) - 2\Psi(1))$ with $J(J + 1) = -(z_1 - z_2)^2 \partial_{z_1} \partial_{z_2}$

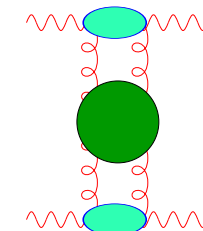
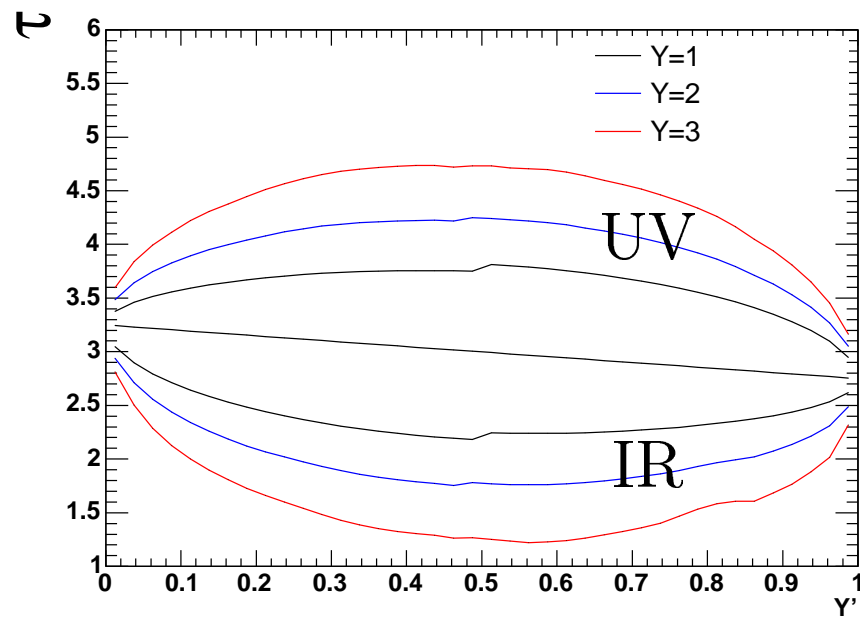
The amplitude for the exchange of N reggeized gluons in the large N_c limit is equivalent to the spin $s = 0$ limit of the Heisenberg ferromagnet.



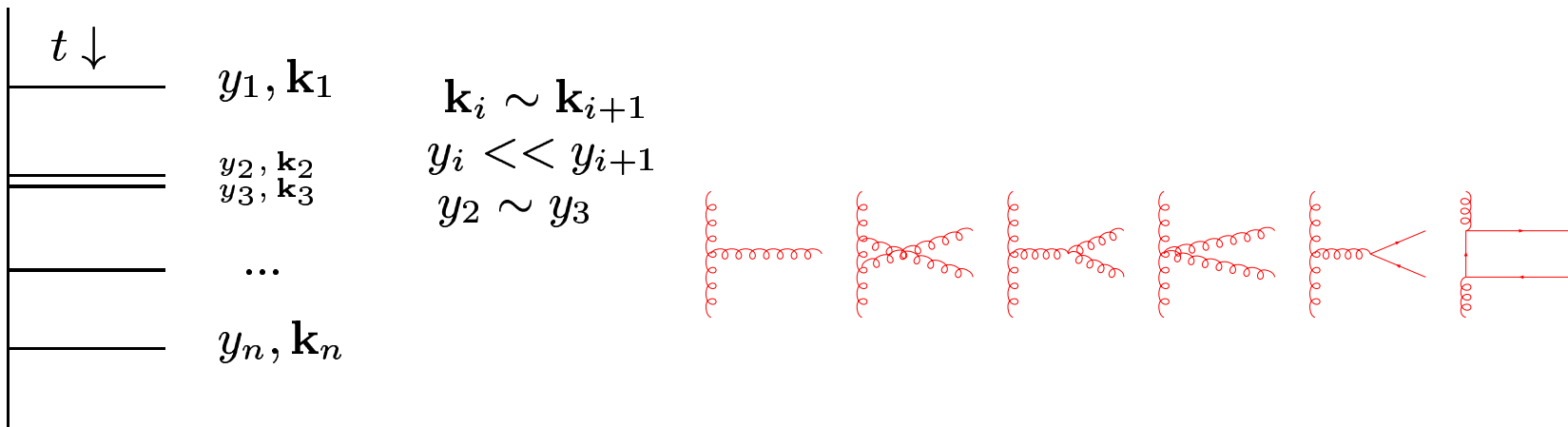
Described by the BKP equation.

Drawbacks of LL approximation:

- Intercept is too large when compared with experiment
- α_s is a fixed constant
- s_0 is arbitrary
- Diffusion of internal momenta into the infrared region.



To run the coupling & fix the energy scale in Y:
 quasi–multiRegge kinematics



NLL BFKL Equation: $(\alpha_S Y)^n + \alpha_S (\alpha_S Y)^n$

$$\sigma(s) = \int \frac{d^2 \mathbf{k}_a}{\mathbf{k}_a^2} \int \frac{d^2 \mathbf{k}_b}{\mathbf{k}_b^2} \Phi_A(\mathbf{k}_a) \Phi_B(\mathbf{k}_b) \mathbf{f}(\mathbf{k}_a, \mathbf{k}_b, Y)$$

$$\omega f_\omega(\mathbf{k}_a, \mathbf{k}_b) = \delta^{(2+2\epsilon)}(\mathbf{k}_a - \mathbf{k}_b) + \int d^{2+2\epsilon} \mathbf{k} \mathcal{K}(\mathbf{k}_a, \mathbf{k}) f_\omega(\mathbf{k}, \mathbf{k}_b)$$



2. Iterative view of the BFKL equation



2. Iterative view of the BFKL equation

In **dimension regularisation** the equation reads

$$\omega f_\omega(\mathbf{k}_a, \mathbf{k}_b) = \delta^{(2+2\epsilon)}(\mathbf{k}_a - \mathbf{k}_b) + \int d^{2+2\epsilon} \mathbf{k}' \mathcal{K}(\mathbf{k}_a, \mathbf{k}') f_\omega(\mathbf{k}', \mathbf{k}_b)$$

with kernel

$$\mathcal{K}(\mathbf{k}_a, \mathbf{k}) = 2\omega^{(\epsilon)}(\mathbf{k}_a^2) \delta^{(2+2\epsilon)}(\mathbf{k}_a - \mathbf{k}) + \mathcal{K}_r(\mathbf{k}_a, \mathbf{k})$$

$\mathbf{k} = \mathbf{k}' - \mathbf{k}_a$ shift and split the kernel:

$$\begin{aligned} \omega f_\omega(\mathbf{k}_a, \mathbf{k}_b) &= \delta^{(2+2\epsilon)}(\mathbf{k}_a - \mathbf{k}_b) + \int d^{2+2\epsilon} \mathbf{k} 2\omega^{(\epsilon)}(\mathbf{k}_a^2) \delta^{(2+2\epsilon)}(\mathbf{k}_a - \mathbf{k}) f_\omega(\mathbf{k}, \mathbf{k}_b) \\ &+ \int d^{2+2\epsilon} \mathbf{k} \mathcal{K}_r^{(\epsilon)}(\mathbf{k}_a, \mathbf{k}_a + \mathbf{k}) f_\omega(\mathbf{k}_a + \mathbf{k}, \mathbf{k}_b) + \int d^2 \mathbf{k} \tilde{\mathcal{K}}_r(\mathbf{k}_a, \mathbf{k}_a + \mathbf{k}) f_\omega(\mathbf{k}_a + \mathbf{k}, \mathbf{k}_b) \end{aligned}$$

To cancel the ϵ poles split the integral over \mathbf{k}_t space for $\mathcal{K}_r^{(\epsilon)}$ using a phase space slicing parameter λ ...

2. Iterative view of the BFKL equation

λ appears in the ϵ -dependent real emission:

$$\begin{aligned} \omega f_\omega(\mathbf{k}_a, \mathbf{k}_b) &= \delta^{(2+2\epsilon)}(\mathbf{k}_a - \mathbf{k}_b) + \int d^{2+2\epsilon} \mathbf{k} 2\omega^{(\epsilon)}(\mathbf{k}_a^2) \delta^{(2+2\epsilon)}(\mathbf{k}_a - \mathbf{k}) f_\omega(\mathbf{k}, \mathbf{k}_b) \\ &+ \int d^{2+2\epsilon} \mathbf{k} \mathcal{K}_r^{(\epsilon)}(\mathbf{k}_a, \mathbf{k}_a + \mathbf{k}) \underbrace{\left(\theta(\mathbf{k}^2 - \lambda^2) + \theta(\lambda^2 - \mathbf{k}^2) \right)}_{\mathcal{K}_r(\mathbf{k}_a, \mathbf{k}_a + \mathbf{k})} f_\omega(\mathbf{k}_a + \mathbf{k}, \mathbf{k}_b) \\ &+ \int d^{2+2\epsilon} \mathbf{k} \tilde{\mathcal{K}}_r(\mathbf{k}_a, \mathbf{k}_a + \mathbf{k}) f_\omega(\mathbf{k}_a + \mathbf{k}, \mathbf{k}_b) \end{aligned}$$

$f_\omega(\mathbf{k}_a + \mathbf{k}, \mathbf{k}_b) \simeq f_\omega(\mathbf{k}_a, \mathbf{k}_b)$ for $|\mathbf{k}| < \lambda$ is valid for large $|\mathbf{k}_a|$ & small λ .
small

$$\begin{aligned} \omega f_\omega(\mathbf{k}_a, \mathbf{k}_b) &= \delta^{(2+2\epsilon)}(\mathbf{k}_a - \mathbf{k}_b) \\ &+ \left\{ 2\omega^{(\epsilon)}(\mathbf{k}_a^2) + \int d^{2+2\epsilon} \mathbf{k} \mathcal{K}_r^{(\epsilon)}(\mathbf{k}_a, \mathbf{k}_a + \mathbf{k}) \underbrace{\theta(\lambda^2 - \mathbf{k}^2)}_{\mathcal{K}_r(\mathbf{k}_a, \mathbf{k}_a + \mathbf{k})} \right\} f_\omega(\mathbf{k}_a, \mathbf{k}_b) \\ &+ \int d^{2+2\epsilon} \mathbf{k} \left\{ \mathcal{K}_r^{(\epsilon)}(\mathbf{k}_a, \mathbf{k}_a + \mathbf{k}) \underbrace{\theta(\mathbf{k}^2 - \lambda^2)}_{\tilde{\mathcal{K}}_r(\mathbf{k}_a, \mathbf{k}_a + \mathbf{k})} + \tilde{\mathcal{K}}_r(\mathbf{k}_a, \mathbf{k}_a + \mathbf{k}) \right\} f_\omega(\mathbf{k}_a + \mathbf{k}, \mathbf{k}_b) \end{aligned}$$

What about the ϵ poles? ...

2. Iterative view of the BFKL equation

The gluon Regge trajectory reads

$$2\omega^{(\epsilon)}(\mathbf{q}^2) = -\bar{\alpha}_s \frac{\Gamma(1-\epsilon)}{(4\pi)^\epsilon} \left(\frac{1}{\epsilon} + \ln \frac{q^2}{\mu^2} \right) - \frac{\bar{\alpha}_s^2}{8} \frac{\Gamma^2(1-\epsilon)}{(4\pi)^{2\epsilon}} \left\{ \frac{\beta_0}{N_c} \left(\frac{1}{\epsilon^2} + \ln^2 \frac{q^2}{\mu^2} \right) + \left(\frac{4}{3} - \frac{\pi^2}{3} + \frac{5}{3} \frac{\beta_0}{N_c} \right) \left(\frac{1}{\epsilon} + 2 \ln \frac{q^2}{\mu^2} \right) - \frac{32}{9} + 2\zeta(3) - \frac{28}{9} \frac{\beta_0}{N_c} \right\}$$

$$\beta_0 \equiv \frac{11}{3} N_c - \frac{2}{3} n_f, \quad \bar{\alpha}_s \equiv \frac{\alpha_s(\mu) N_c}{\pi}, \quad \mu \text{ is the } \overline{\text{MS}} \text{ scale.}$$

Integrating ϵ -dependent real emission ...

$$\int d^{2+2\epsilon} \mathbf{k} \mathcal{K}_r^{(\epsilon)}(\mathbf{q}, \mathbf{q} + \mathbf{k}) \theta(\lambda^2 - \mathbf{k}^2) = \frac{1}{\Gamma(1+\epsilon)} \frac{\bar{\alpha}_s}{(4\pi)^\epsilon} \frac{1}{\epsilon} \left(\frac{\lambda^2}{\mu^2} \right)^\epsilon$$

$$\left\{ 1 + \frac{\bar{\alpha}_s}{4} \frac{\Gamma(1-\epsilon)}{(4\pi)^\epsilon} \left[\frac{\beta_0}{N_c} \frac{1}{\epsilon} \left(1 - \frac{1}{2} \left(\frac{\lambda^2}{\mu^2} \right)^\epsilon \left(1 - \epsilon^2 \frac{\pi^2}{6} \right) \right) \right. \right.$$

$$\left. \left. + \frac{1}{2} \left(\frac{\lambda^2}{\mu^2} \right)^\epsilon \left(\frac{4}{3} - \frac{\pi^2}{3} + \frac{5}{3} \frac{\beta_0}{N_c} + \epsilon \left(-\frac{32}{9} + 14\zeta(3) - \frac{28}{9} \frac{\beta_0}{N_c} \right) \right) \right] \right\}$$

We can now combine these two results ...

2. Iterative view of the BFKL equation

$$\mathcal{K}(\mathbf{k}_a, \mathbf{k}) = 2\omega^{(\epsilon)}(\mathbf{k}_a) \delta^{(2+2\epsilon)}(\mathbf{k}_a - \mathbf{k}) + \mathcal{K}_r(\mathbf{k}_a, \mathbf{k})$$

Regularise the gluon Regge trajectory as

$$\begin{aligned} \omega_\lambda(\mathbf{q}) &\equiv \lim_{\epsilon \rightarrow 0} \left\{ 2\omega^{(\epsilon)}(\mathbf{q}) + \int d^{2+2\epsilon}\mathbf{k} \mathcal{K}_r^{(\epsilon)}(\mathbf{q}, \mathbf{q} + \mathbf{k}) \theta(\lambda^2 - \mathbf{k}^2) \right\} = \\ &- \bar{\alpha}_s \left\{ \ln \frac{\mathbf{q}^2}{\lambda^2} + \frac{\bar{\alpha}_s}{4} \left[\frac{\beta_0}{2N_c} \ln \frac{\mathbf{q}^2}{\lambda^2} \ln \frac{\mu^4}{\mathbf{q}^2 \lambda^2} + \left(\frac{4}{3} - \frac{\pi^2}{3} + \frac{5}{3} \frac{\beta_0}{N_c} \right) \ln \frac{\mathbf{q}^2}{\lambda^2} - 6\zeta(3) \right] \right\} \end{aligned}$$

Very simple!:

$$\omega_\lambda(\mathbf{q}) = - \int_{\lambda^2}^{\mathbf{q}^2} \frac{d\mathbf{k}^2}{\mathbf{k}^2} (\bar{\alpha}_s(k^2) + \bar{\alpha}_s^2 \mathcal{S}) + \text{constant}$$

$$\mathcal{S} = \frac{1}{3} - \frac{\pi^2}{12} + \frac{5}{12} \frac{\beta_0}{N_c} \quad \text{constant} = \bar{\alpha}_s^2 \frac{3}{2} \zeta(3)$$

2. Iterative view of the BFKL equation

The NLL BFKL equation then reads

$$(\omega - \omega_\lambda(\mathbf{k}_a)) f_\omega(\mathbf{k}_a, \mathbf{k}_b) = \delta^{(2)}(\mathbf{k}_a - \mathbf{k}_b) + \int d^2\mathbf{k} \left(\frac{\xi(\mathbf{k}^2)}{\pi\mathbf{k}^2} \theta(\mathbf{k}^2 - \lambda^2) + \tilde{\mathcal{K}}_r(\mathbf{k}_a, \mathbf{k}_a + \mathbf{k}) \right) f_\omega(\mathbf{k}_a + \mathbf{k}, \mathbf{k}_b)$$

where

$$\xi(X) = \bar{\alpha}_s + \frac{\bar{\alpha}_s^2}{4} \left(\frac{4}{3} - \frac{\pi^2}{3} + \frac{5}{3} \frac{\beta_0}{N_c} - \frac{\beta_0}{N_c} \ln \frac{X}{\mu^2} \right)$$

In this notation:

$$\omega_\lambda(\mathbf{q}) = - \int_{\lambda^2}^{\mathbf{q}^2} \frac{d\mathbf{k}^2}{\mathbf{k}^2} \xi(\mathbf{k}^2) + \text{constant}$$

Ensuring the λ -independence of the equation...

2. Iterative view of the BFKL equation

The equation can be iterated using the initial condition:

$$\begin{aligned}
 f_\omega(\mathbf{k}_a, \mathbf{k}_b) &= \frac{\delta^{(2)}(\mathbf{k}_a - \mathbf{k}_b)}{\omega - \omega_\lambda(\mathbf{k}_a)} + \int d^2\mathbf{k}_1 \frac{\hat{\mathcal{K}}_r^\lambda(\mathbf{k}_a, \mathbf{k}_a + \mathbf{k}_1)}{\omega - \omega_\lambda(\mathbf{k}_a)} \frac{\delta^{(2)}(\mathbf{k}_a + \mathbf{k}_1 - \mathbf{k}_b)}{\omega - \omega_\lambda(\mathbf{k}_a + \mathbf{k}_1)} \\
 &+ \int d^2\mathbf{k}_1 \frac{\hat{\mathcal{K}}_r^\lambda(\mathbf{k}_a, \mathbf{k}_a + \mathbf{k}_1)}{\omega - \omega_\lambda(\mathbf{k}_a)} \\
 &\quad \int d^2\mathbf{k}_2 \frac{\hat{\mathcal{K}}_r^\lambda(\mathbf{k}_a + \mathbf{k}_1, \mathbf{k}_a + \mathbf{k}_1 + \mathbf{k}_2)}{\omega - \omega_\lambda(\mathbf{k}_a + \mathbf{k}_1)} \frac{\delta^{(2)}(\mathbf{k}_a + \mathbf{k}_1 + \mathbf{k}_2 - \mathbf{k}_b)}{\omega - \omega_\lambda(\mathbf{k}_a + \mathbf{k}_1 + \mathbf{k}_2)} \\
 &+ \dots
 \end{aligned}$$

and Mellin transform back into energy space:

$$\textcolor{blue}{f}(\mathbf{k}_a, \mathbf{k}_b, Y) = \frac{1}{2\pi i} \int_{a-i\infty}^{a+i\infty} d\omega e^{\omega Y} f_\omega(\mathbf{k}_a, \mathbf{k}_b)$$

finally ...

2. Iterative view of the BFKL equation

... the NLL BFKL gluon Green's function reads

$$\begin{aligned}
 \textcolor{blue}{f}(\mathbf{k}_a, \mathbf{k}_b, Y) &= e^{(\omega_\lambda(\mathbf{k}_a)Y)} \left\{ \delta^{(2)}(\mathbf{k}_a - \mathbf{k}_b) \right. \\
 &+ \sum_{n=1}^{\infty} \prod_{i=1}^n \int d^2 \mathbf{k}_i \left[\frac{\theta(\mathbf{k}_i^2 - \lambda^2)}{\pi \mathbf{k}_i^2} \xi(\mathbf{k}_i^2) + \tilde{\mathcal{K}}_r \left(\mathbf{k}_a + \sum_{l=0}^{i-1} \mathbf{k}_l, \mathbf{k}_a + \sum_{l=1}^i \mathbf{k}_l \right) \right] \\
 &\times \left. \int_0^{y_{i-1}} dy_i \ e^{\left(\omega_\lambda \left(\mathbf{k}_a + \sum_{l=1}^i \mathbf{k}_l \right) - \omega_\lambda \left(\mathbf{k}_a + \sum_{l=1}^{i-1} \mathbf{k}_l \right) \right) y_i} \delta^{(2)} \left(\sum_{l=1}^n \mathbf{k}_l + \mathbf{k}_a - \mathbf{k}_b \right) \right\}
 \end{aligned}$$

with $y_0 \equiv Y$.

2. Iterative view of the BFKL equation

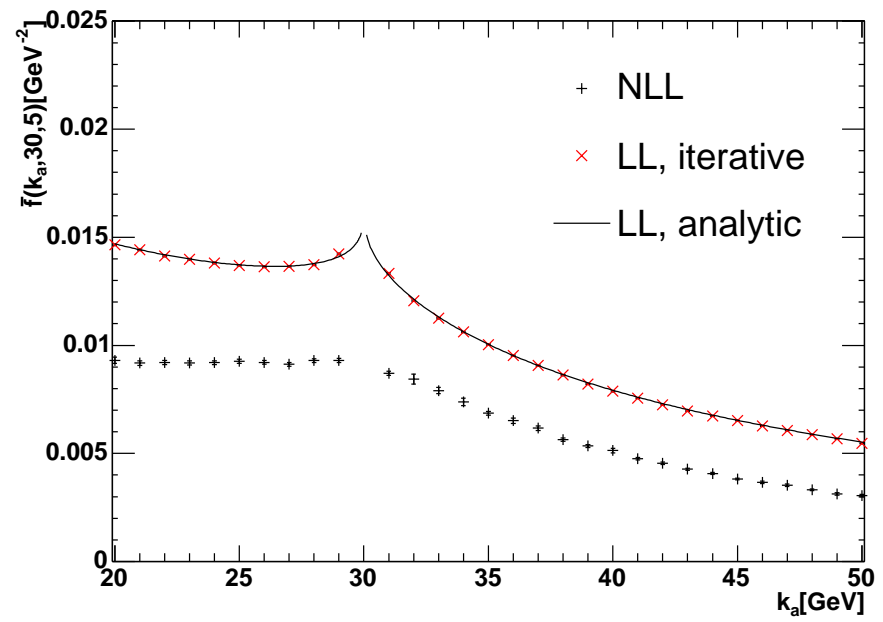
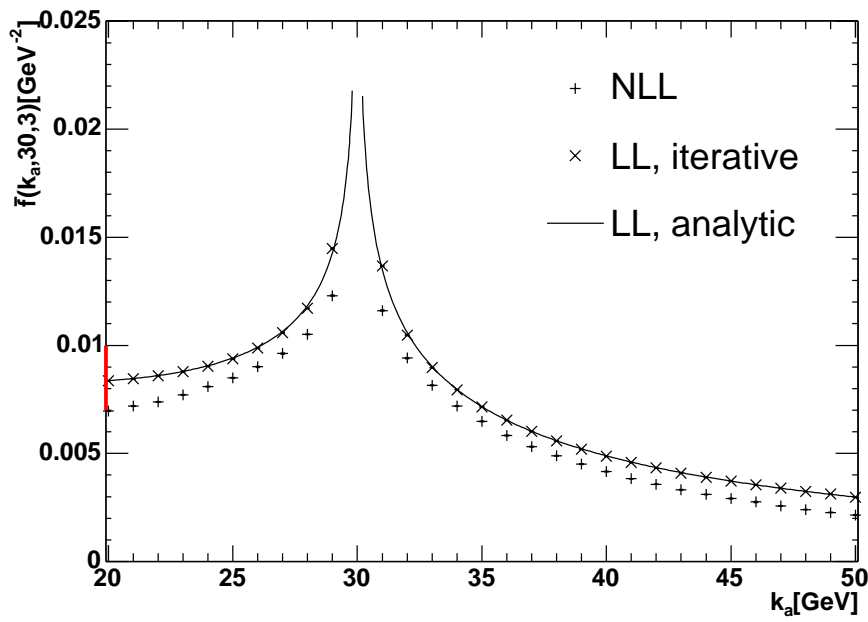
The LL limit agrees with

$$\begin{aligned}\omega_0(\mathbf{q}^2, \lambda) &= -\bar{\alpha}_s \ln \frac{\mathbf{q}^2}{\lambda^2} \\ \xi &= \bar{\alpha}_s \\ \eta &= 0 \\ \tilde{\mathcal{K}}_r(\mathbf{q}, \mathbf{q}') &= 0\end{aligned}$$

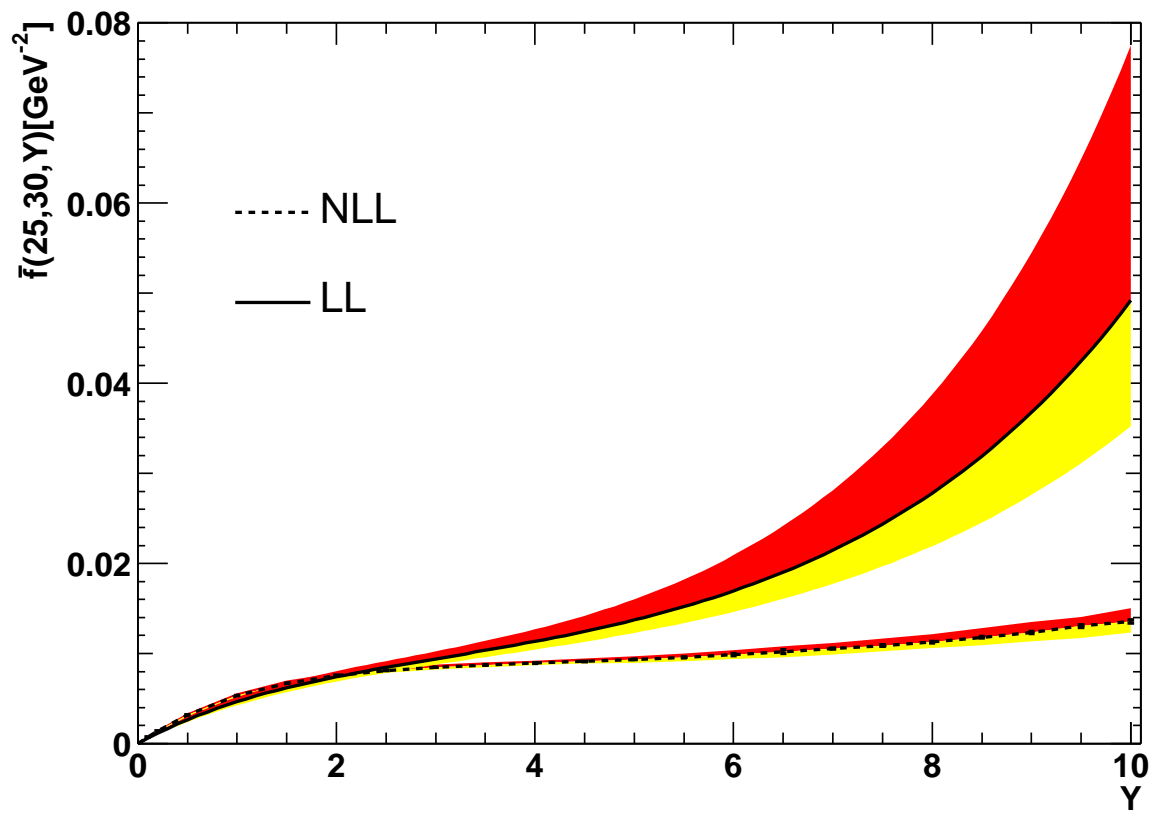
and the solution is very simple

$$\begin{aligned}f(\mathbf{k}_a, \mathbf{k}_b, Y) &= \left(\frac{\lambda^2}{k_a^2} \right)^{\bar{\alpha}_s Y} \left\{ \delta^{(2)}(\mathbf{k}_a - \mathbf{k}_b) \right. \\ &+ \sum_{n=1}^{\infty} \prod_{i=1}^n \bar{\alpha}_s \int d^2 \mathbf{k}_i \frac{\theta(\mathbf{k}_i^2 - \lambda^2)}{\pi \mathbf{k}_i^2} \\ &\quad \left. \int_0^{y_{i-1}} dy_i \left(\frac{(\mathbf{k}_a + \sum_{l=1}^{i-1} \mathbf{k}_l)^2}{(\mathbf{k}_a + \sum_{l=1}^i \mathbf{k}_l)^2} \right)^{\bar{\alpha}_s y_i} \delta^{(2)} \left(\sum_{l=1}^n \mathbf{k}_l + \mathbf{k}_a - \mathbf{k}_b \right) \right\}\end{aligned}$$

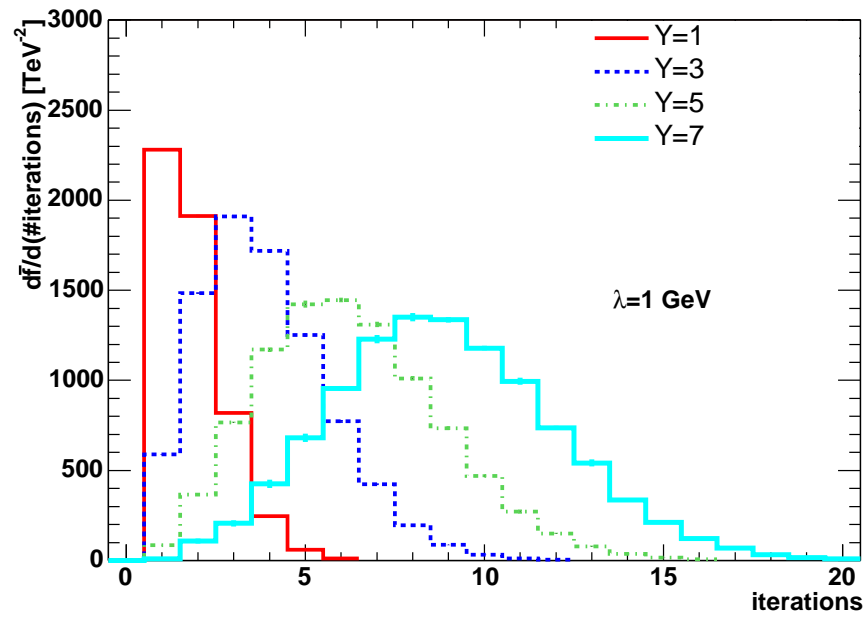
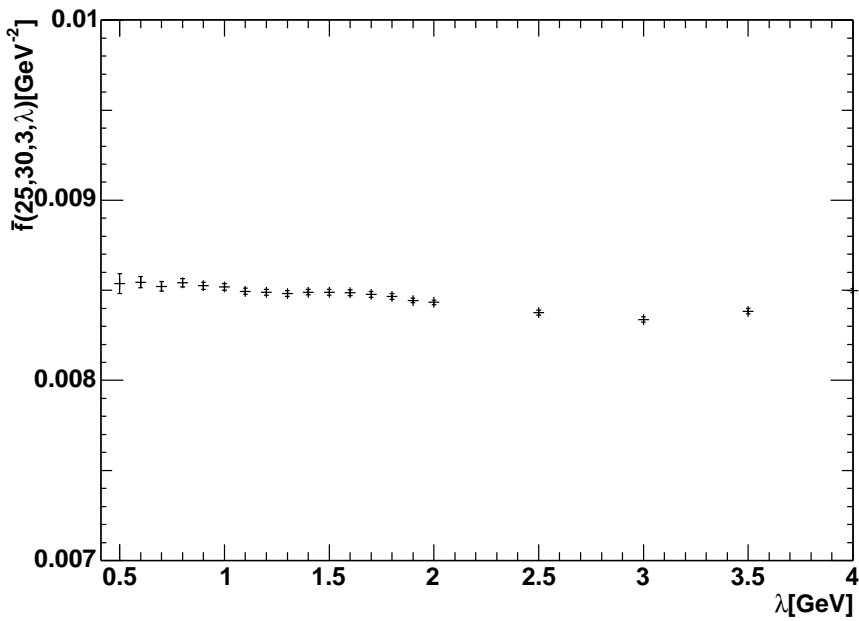
2. Iterative view of the BFKL equation



2. Iterative view of the BFKL equation

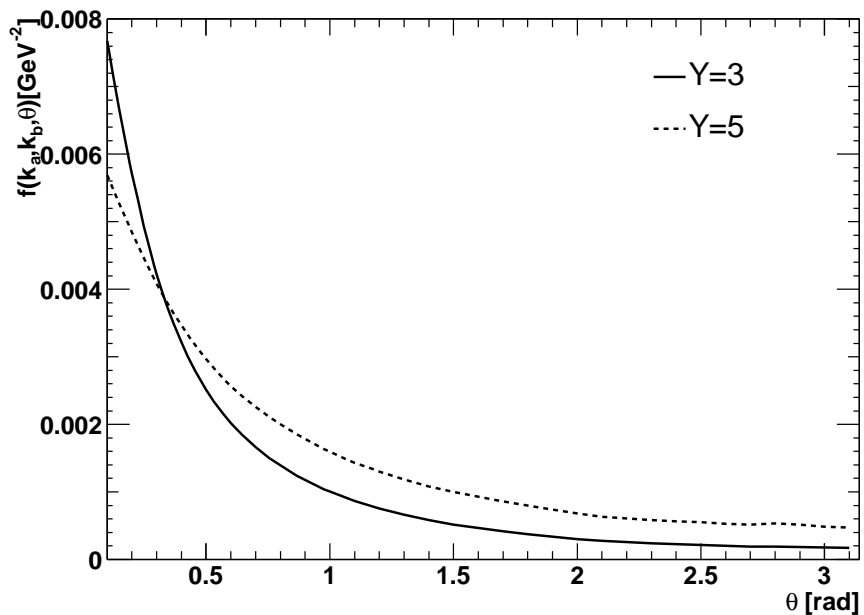


2. Iterative view of the BFKL equation

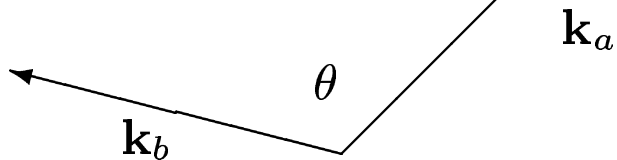


2. Iterative view of the BFKL equation

Angular correlations can be studied:

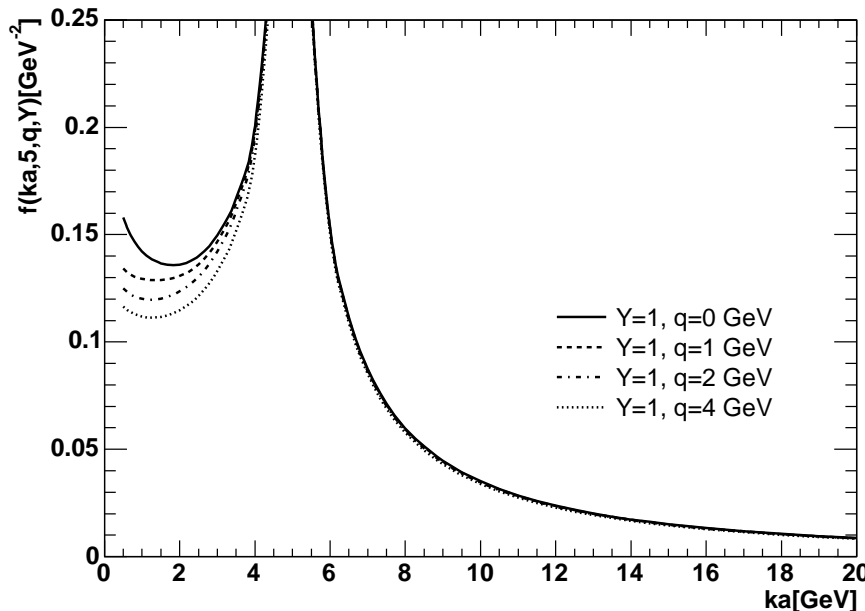
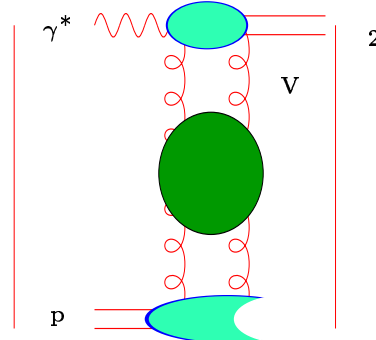


$$k_a = 25 \text{ GeV}, k_b = 30 \text{ GeV}.$$



2. Iterative view of the BFKL equation

Momentum transfer $q \neq 0$: Diffractive events with Rapidity Gaps



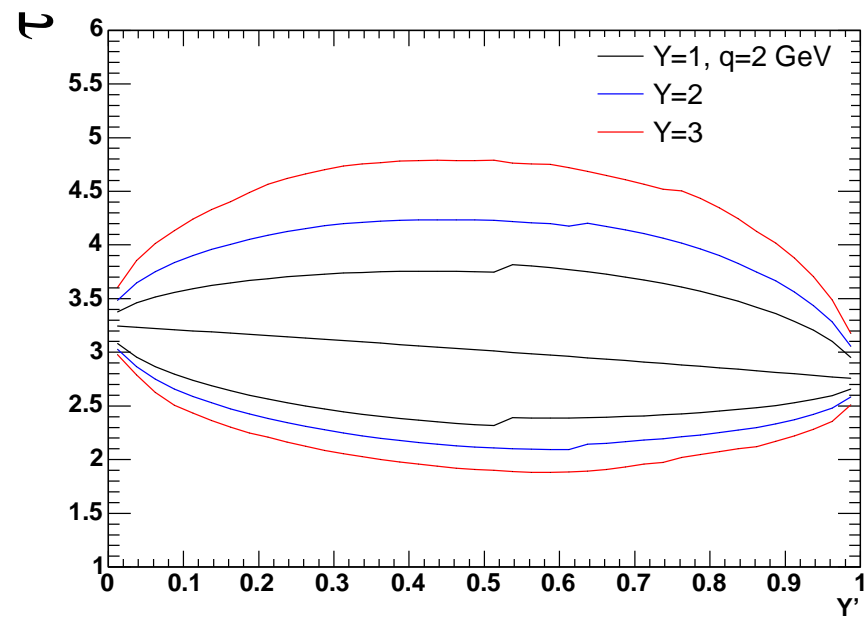
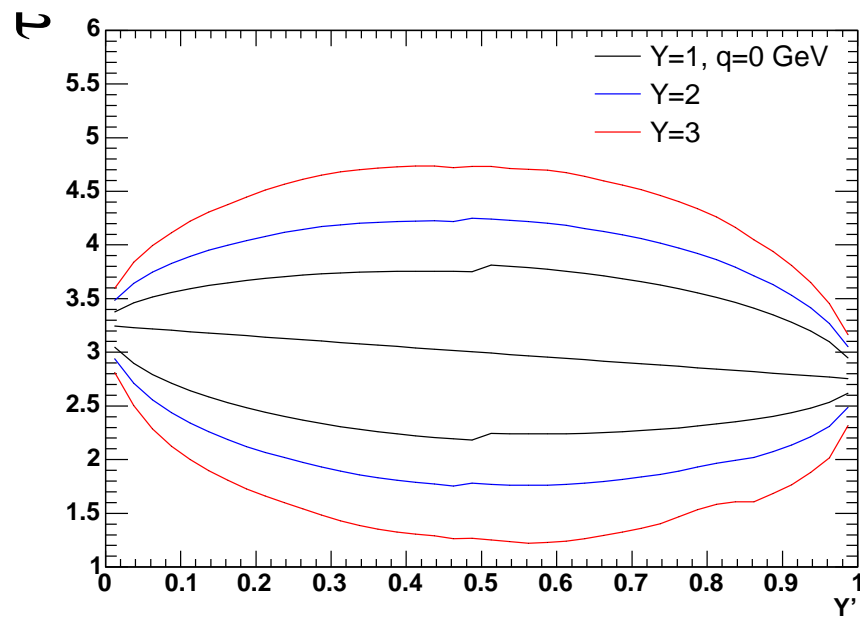
LL analysis:

$$\omega_\lambda(\mathbf{k}_a, \mathbf{q}) = -\frac{\bar{\alpha}_s}{2} \left(\ln \frac{\mathbf{k}_a^2}{\lambda^2} + \ln \frac{(\mathbf{k}_a - \mathbf{q})^2}{\lambda^2} \right)$$

$$\xi(\mathbf{k}_a, \mathbf{k}, \mathbf{q}) = \frac{\bar{\alpha}_s}{2} \left(1 + \frac{(\mathbf{k}_a - \mathbf{q})^2 (\mathbf{k} + \mathbf{k}_a)^2 - \mathbf{q}^2 \mathbf{k}^2}{(\mathbf{k} + \mathbf{k}_a - \mathbf{q})^2 \mathbf{k}_a^2} \right)$$

2. Iterative view of the BFKL equation

Diffusion into the infrared is cut-off by the momentum transfer, typical transverse momenta:



2. Iterative view of the BFKL equation

Non-forward NLL BFKL kernel can be studied in the same way ...

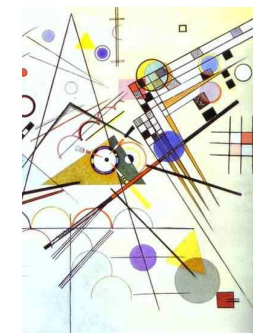
$$\begin{aligned} \omega_\lambda(\mathbf{k}_a, \mathbf{q}) = & -\frac{1}{2} \left\{ \bar{\alpha}_s + \frac{\bar{\alpha}_s^2}{4} \left[\mathcal{S} - \frac{\beta_0}{2N_c} \ln \frac{\mathbf{k}_a^2 \lambda^2}{\mu^4} \right] \right\} \ln \frac{\mathbf{k}_a^2}{\lambda^2} + 3\zeta(3)\bar{\alpha}_s^2 \\ & -\frac{1}{2} \left\{ \bar{\alpha}_s + \frac{\bar{\alpha}_s^2}{4} \left[\mathcal{S} - \frac{\beta_0}{2N_c} \ln \frac{(\mathbf{k}_a - \mathbf{q})^2 \lambda^2}{\mu^4} \right] \right\} \ln \frac{(\mathbf{k}_a - \mathbf{q})^2}{\lambda^2} \end{aligned}$$

$$\xi(\mathbf{k}_a, \mathbf{k}, \mathbf{q}) = \frac{\bar{\alpha}_s}{2} \left(1 + \frac{(\mathbf{k}_a - \mathbf{q})^2 (\mathbf{k}_a + \mathbf{k})^2 - \mathbf{q}^2 \mathbf{k}^2}{\mathbf{k}_a^2 (\mathbf{k}_a - \mathbf{q} + \mathbf{k})^2} \right) \left\{ 1 + \frac{\bar{\alpha}_s}{4} \left(\mathcal{S} - \frac{\beta_0}{N_c} \ln \frac{\mathbf{k}^2}{\mu^2} \right) \right\}$$

The remaining parts of the kernel are a bit more complicated ...

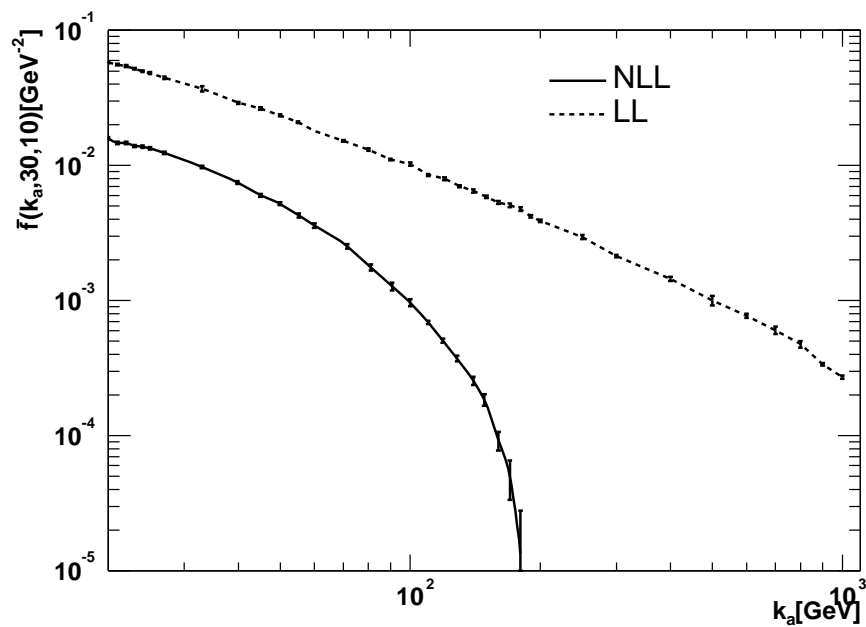


3. Short range correlations



3. Short range correlations

Forward case: Behaviour for small/large $\frac{k_a}{k_b}$ ratios:



Collinear/Anticollinear limits: Oscillations

What is happening?

3. Short range correlations

- Gluon trajectory $\omega(k_a^2)$
 - Emission kernel $K_r(k_a, k)$
- which can be expanded in perturbation theory

$$\begin{aligned} \mathcal{K}(k_a, k) &= 2 \left\{ \omega^{\text{LL}}(k_a^2) + \omega^{\text{NLL}}(k_a^2) + \dots \right\} \delta^{(2)}(k_a - k) \\ &\quad + K_r^{\text{LL}}(k_a, k) + K_r^{\text{NLL}}(k_a, k) + \dots \end{aligned}$$

What can we do analytically?

$$\begin{aligned} \int d^2k \mathcal{K}(k_a, k) \left(\frac{k^2}{k_a^2} \right)^{\gamma-1} &= \left\{ \bar{\alpha}_s(\mu^2) \chi^{\text{LL}}(\gamma) + \bar{\alpha}_s^2(\mu^2) \chi^{\text{NLL}}(\gamma) \right\}_{\text{Scale invariant}} \\ &\quad - \left\{ \bar{\alpha}_s^2(\mu^2) \chi^{\text{LL}}(\gamma) \frac{\beta_0}{4N_c} \ln \frac{k_a^2}{\mu^2} \right\}_{\text{Running Coupling}} \end{aligned}$$

3. Short range correlations

Let's introduce a separation in rapidity space

We don't allow two emissions to have very similar rapidity

$$\mathbf{k}_i \sim \mathbf{k}_{i+1}$$

$$y_i \ll y_{i+1}$$

$$y_{i+1} - y_i > b$$

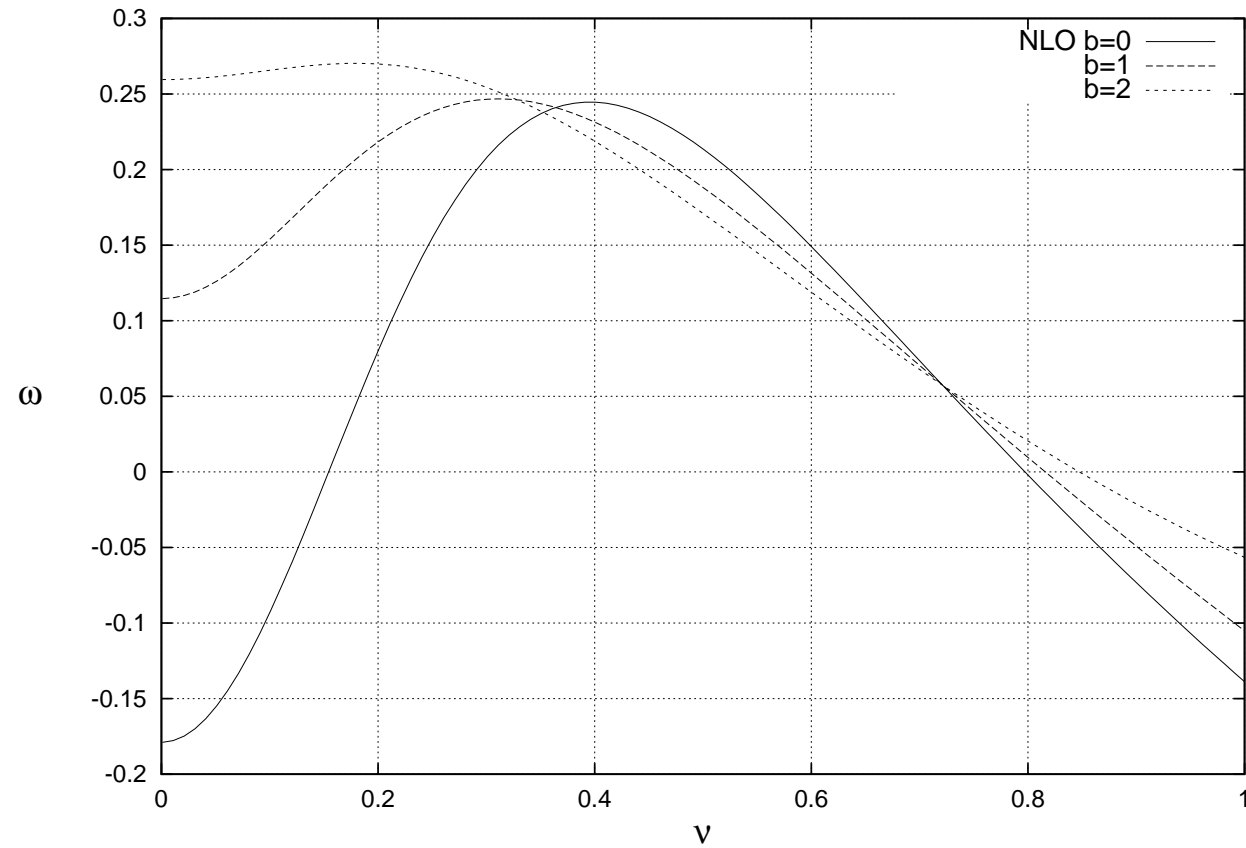
$$\alpha_s^n \int_0^Y dy_1 \int_0^{y_1-b} dy_2 \dots \int_0^{y_{n-1}-b} dy_n \sim \frac{(\alpha_s \chi_0(\gamma)(Y - nb))^n}{n!}$$

It should match NLL accuracy ...

$$\omega = \bar{\alpha}_s e^{-b\omega} [\chi_0(\gamma) + \bar{\alpha}_s \chi_1(\gamma) + \bar{\alpha}_s b \chi_0^2(\gamma)]$$

3. Short range correlations

It also solves the problem of the double maxima ...

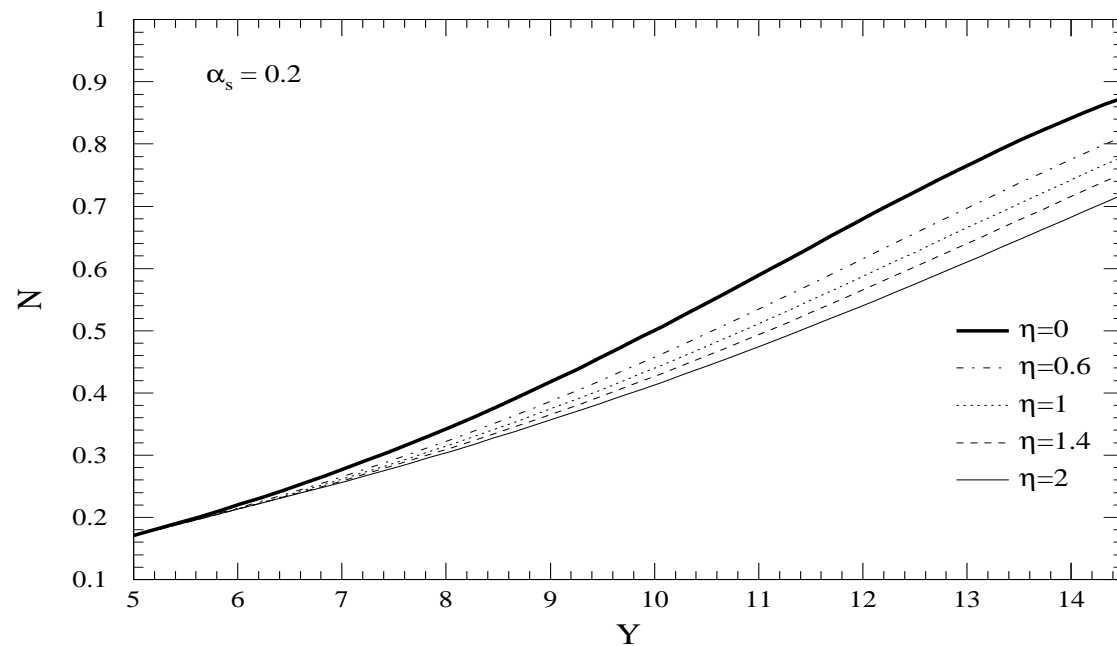


for values of the veto $b \sim 2$.

3. Short range correlations

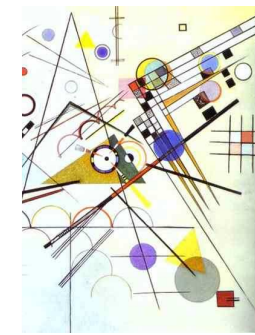
A brief remark: It serves as a reasonable estimate of higher order corrections in Balitsky–Kovchegov eqn for color dipoles ...

$$\frac{dN(\mathbf{x}_{01}, Y)}{dY} = \int_{\rho} \frac{d^2 \mathbf{x}_2}{2 \pi} \frac{\bar{\alpha}_s \mathbf{x}_{01}^2}{\mathbf{x}_{02}^2 \mathbf{x}_{12}^2} [2N(\mathbf{x}_{02}, Y) - N(\mathbf{x}_{01}, Y) - N(\mathbf{x}_{02}, Y)N(\mathbf{x}_{12}, Y)]$$



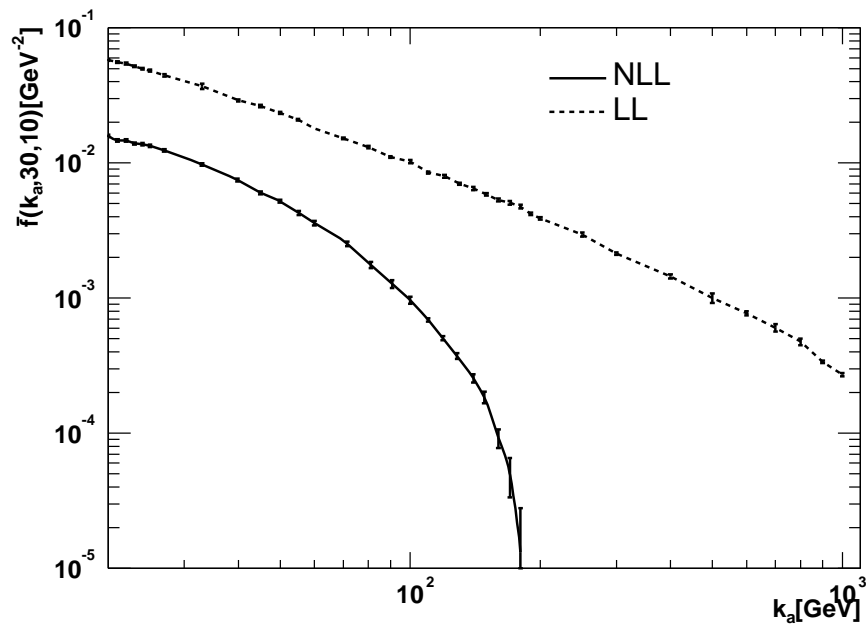


4. A look at renormalization-group improved equation



4. A look at renormalization-group improved equation

Forward case: Behaviour for small/large $\frac{k_a}{k_b}$ ratios:



Collinear/Anticollinear limits: Oscillations

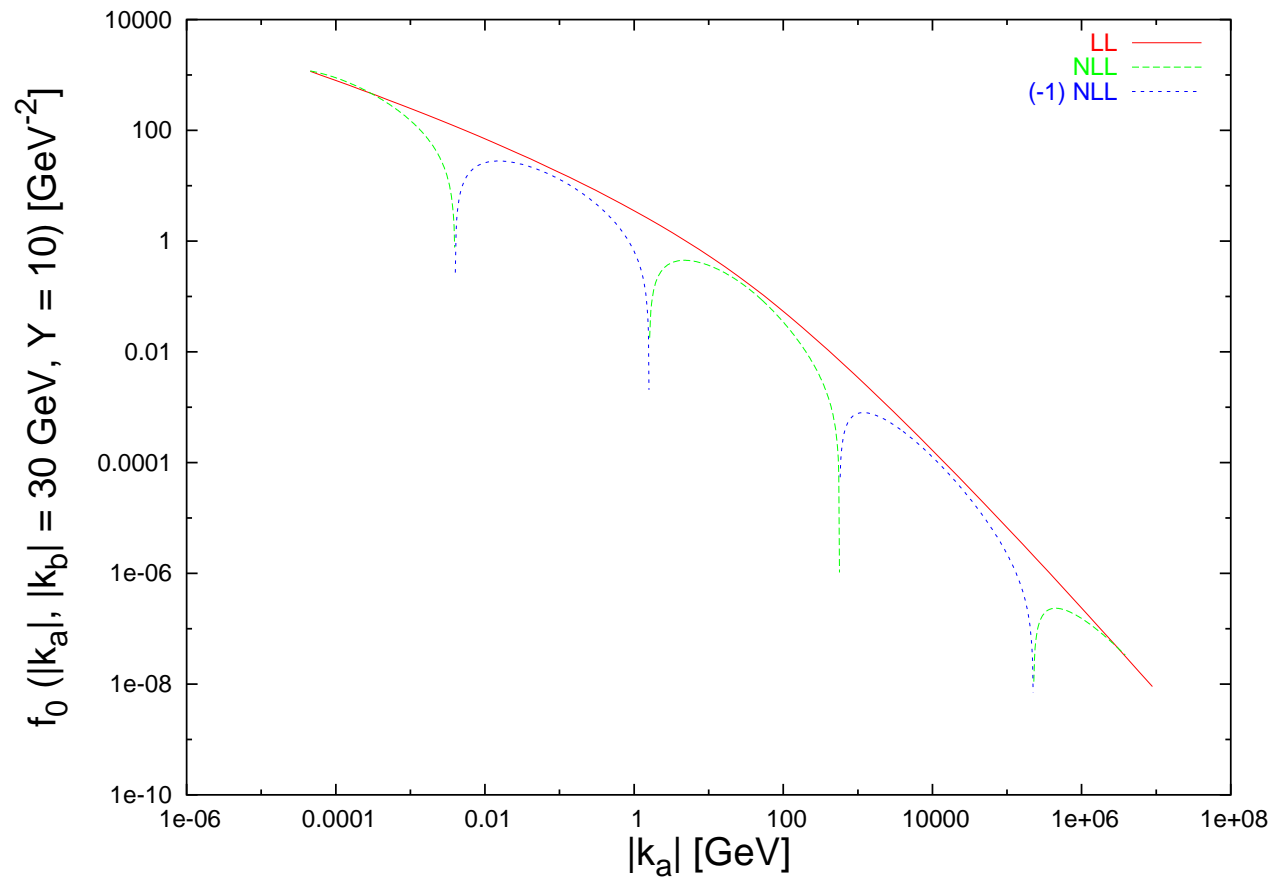
4. A look at renormalization-group improved equation

$$\begin{array}{ccc}
 & \mathbf{k}_i \downarrow y_i & \\
 \mathbf{k}_a + \sum_{l=0}^{i-1} \mathbf{k}_l & \longrightarrow & \longrightarrow \mathbf{k}_a + \sum_{l=1}^i \mathbf{k}_l \\
 \hline
 & \bullet &
 \end{array}$$

$$-\frac{\bar{\alpha}_s^2(\mu)}{4\pi} \frac{1}{\mathbf{k}_i^2} \ln^2 \left(\frac{\left(\mathbf{k}_a + \sum_{l=0}^{i-1} \mathbf{k}_l \right)^2}{\left(\mathbf{k}_a + \sum_{l=1}^i \mathbf{k}_l \right)^2} \right)$$

4. A look at renormalization-group improved equation

The double maxima generate oscillations in \mathbf{k}_t space:



4. A look at renormalization-group improved equation

Origin of the oscillations: $\chi_0(\gamma) = \bar{\alpha}_s (2\Psi(1) - \Psi(\gamma) - \Psi(1-\gamma))$

$$f \sim \int \left(\frac{s}{k_a k_b} \right)^\omega \left(\frac{\mathbf{k}_a^2}{\mathbf{k}_b^2} \right)^{\gamma - \frac{1}{2}} \frac{d\omega d\gamma}{\omega - \chi_0(\gamma)} = \int \left(\frac{s}{k_a^2} \right)^\omega \left(\frac{\mathbf{k}_a^2}{\mathbf{k}_b^2} \right)^{\gamma - \frac{1}{2}} \frac{d\omega d\gamma}{\omega - \chi_0(\gamma - \frac{\omega}{2})}$$

In collinear limit $\gamma \sim 0$: $\omega(\gamma) \sim \frac{\bar{\alpha}_s}{\gamma}$

$$\omega \sim \frac{\bar{\alpha}_s}{\gamma - \frac{\omega}{2}} \longrightarrow \omega \sim \frac{\bar{\alpha}_s}{\gamma} + \frac{\bar{\alpha}_s^2}{2\gamma^3} + \sum_{n=2}^{\infty} \frac{(2n)!}{2^n n! (n+1)!} \frac{\bar{\alpha}_s^{n+1}}{\gamma^{2n+1}}$$

Not allowed by DGLAP. Only the second one cancelled by NLL kernel.

The remaining terms are numerically large.

Proposal: $\chi_0^{\text{new}}(\gamma) \equiv \chi_0\left(\gamma + \frac{\omega}{2}\right)$

$$f \sim \int \left(\frac{s}{k_a k_b} \right)^\omega \left(\frac{\mathbf{k}_a^2}{\mathbf{k}_b^2} \right)^{\gamma - \frac{1}{2}} \frac{d\omega d\gamma}{\omega - \chi_0(\gamma + \frac{\omega}{2})} = \int \left(\frac{s}{k_a^2} \right)^\omega \left(\frac{\mathbf{k}_a^2}{\mathbf{k}_b^2} \right)^{\gamma - \frac{1}{2}} \frac{d\omega d\gamma}{\omega - \chi_0(\gamma)}$$

Collinear limit free from unphysical double logs.

4. A look at renormalization-group improved equation

$$\int d^2\mathbf{q}_2 \mathcal{K}(\mathbf{q}_1, \mathbf{q}_2) \left(\frac{\bar{\alpha}_s(q_2^2)}{\bar{\alpha}_s(q_1^2)} \right)^{-\frac{1}{2}} \left(\frac{q_2^2}{q_1^2} \right)^{\gamma-1} = \bar{\alpha}_s(q_1^2) \chi_0(\gamma) + \bar{\alpha}_s^2 \chi_1(\gamma)$$

$$\chi_0(\gamma) \simeq \frac{1}{\gamma} + \{\gamma \rightarrow 1 - \gamma\}, \quad \chi_1(\gamma) \simeq \frac{a}{\gamma} + \frac{b}{\gamma^2} - \frac{1}{2\gamma^3} + \{\gamma \rightarrow 1 - \gamma\}$$

$$a = \frac{5}{12} \frac{\beta_0}{N_c} - \frac{13}{36} \frac{n_f}{N_c^3} - \frac{55}{36}, \quad b = -\frac{1}{8} \frac{\beta_0}{N_c} - \frac{n_f}{6N_c^3} - \frac{11}{12}.$$

Renormalization-group-improved kernel:

$$\begin{aligned} \omega &= \bar{\alpha}_s \left(1 + \left(a + \frac{\pi^2}{6} \right) \bar{\alpha}_s \right) \left(2\psi(1) - \psi \left(\gamma + \frac{\omega}{2} - b \bar{\alpha}_s \right) - \psi \left(1 - \gamma + \frac{\omega}{2} - b \bar{\alpha}_s \right) \right) \\ &+ \bar{\alpha}_s^2 \left(\chi_1(\gamma) + \left(\frac{1}{2} \chi_0(\gamma) - b \right) \left(\psi'(\gamma) + \psi'(1 - \gamma) \right) - \left(a + \frac{\pi^2}{6} \right) \chi_0(\gamma) \right) \end{aligned}$$

Is there a simple representation in k_t -rapidity space?

4. A look at renormalization-group improved equation

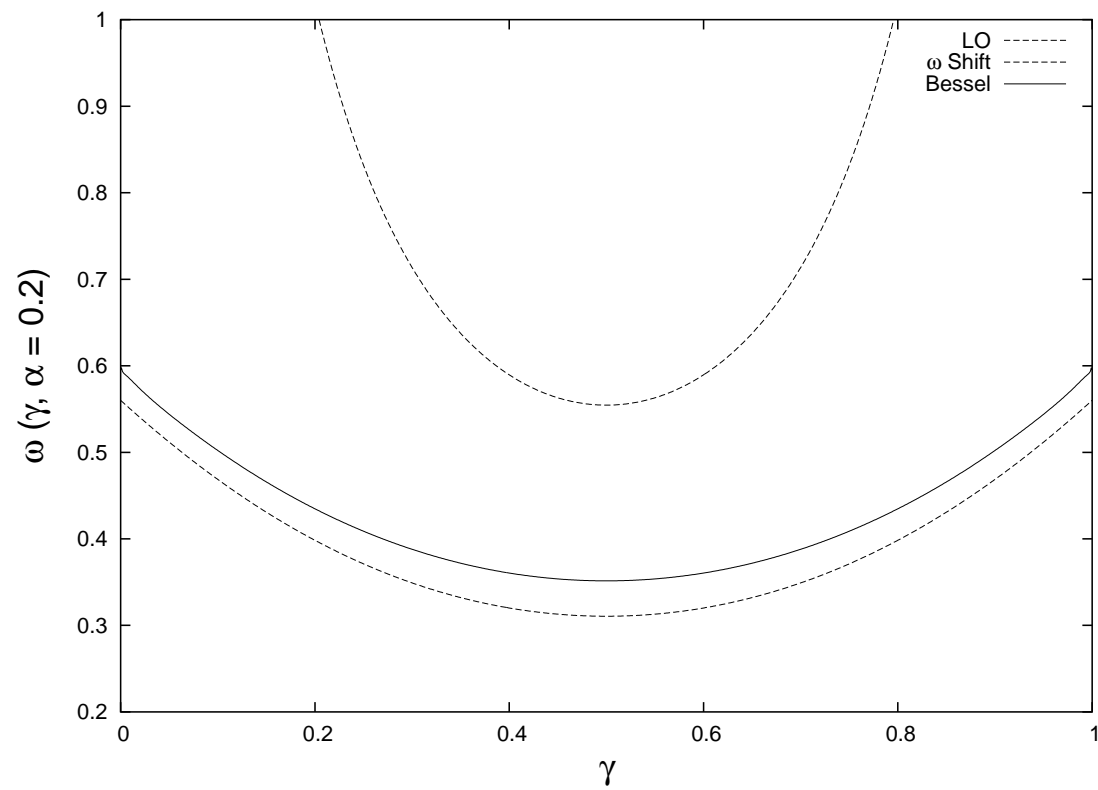
Main idea: the solution to

$$\omega = \bar{\alpha}_s \left(2\psi(1) - \psi\left(\gamma + \frac{\omega}{2}\right) - \psi\left(1 - \gamma + \frac{\omega}{2}\right) \right)$$

at small coupling can be approximated very well by

$$\omega = \int_0^1 \frac{dx}{1-x} \left\{ \left(x^{\gamma-1} + x^{-\gamma} \right) \sqrt{\frac{2\bar{\alpha}_s}{\ln^2 x}} J_1 \left(\sqrt{2\bar{\alpha}_s \ln^2 x} \right) - 2\bar{\alpha}_s \right\}$$

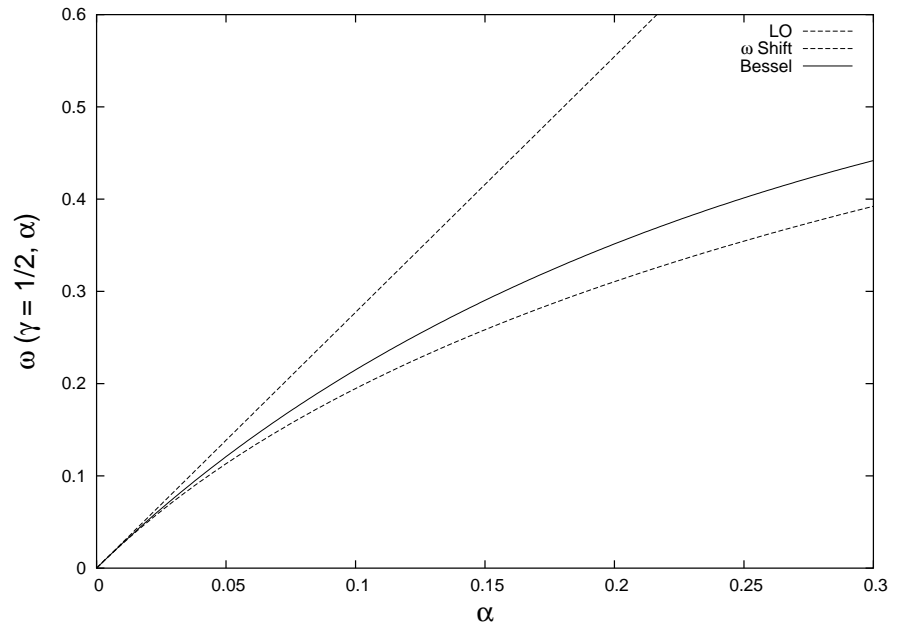
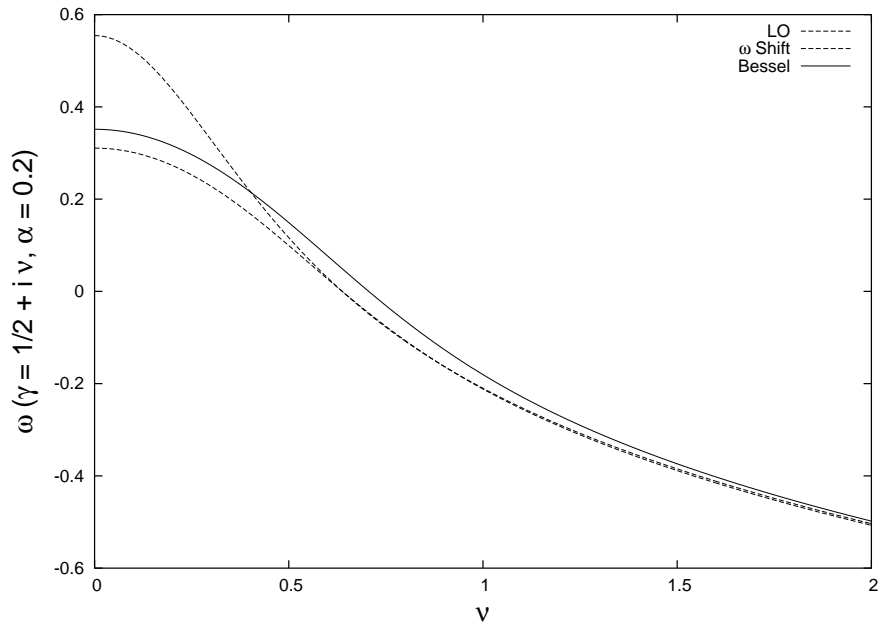
4. A look at renormalization-group improved equation



4. A look at renormalization-group improved equation

$$\omega = \bar{\alpha}_s \left(2\psi(1) - \psi\left(\gamma + \frac{\omega}{2}\right) - \psi\left(1 - \gamma + \frac{\omega}{2}\right) \right)$$

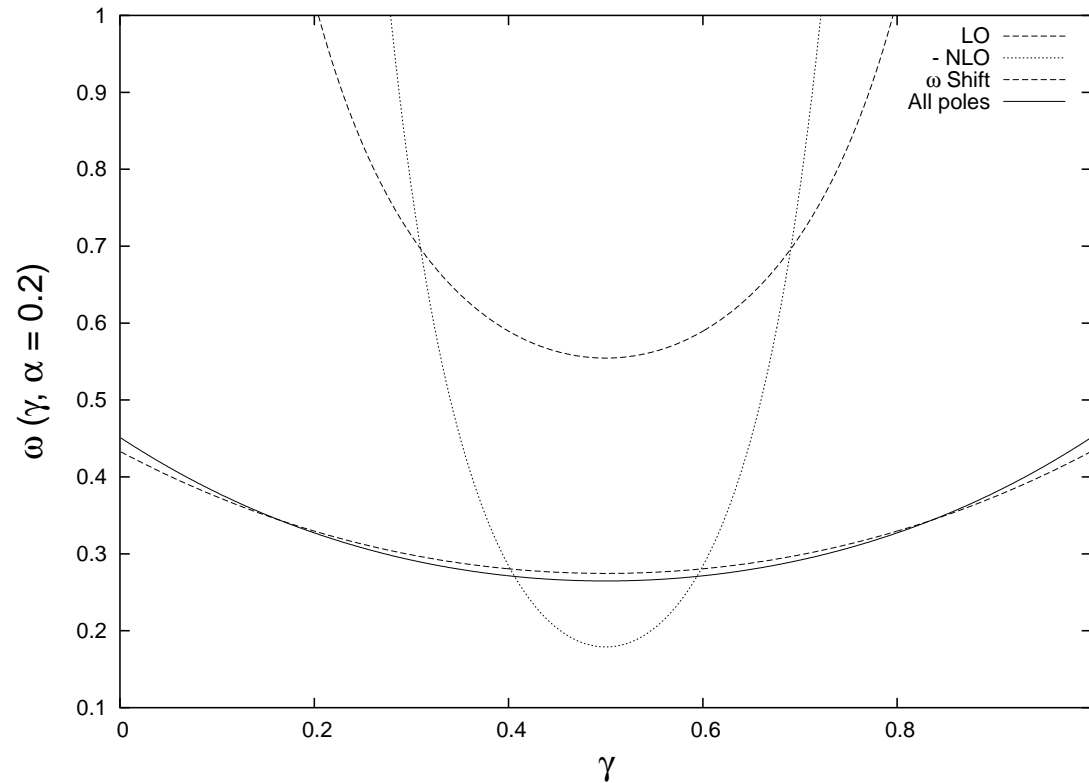
$$\omega = \int_0^1 \frac{dx}{1-x} \left\{ \left(x^{\gamma-1} + x^{-\gamma} \right) \sqrt{\frac{2\bar{\alpha}_s}{\ln^2 x}} J_1 \left(\sqrt{2\bar{\alpha}_s \ln^2 x} \right) - 2\bar{\alpha}_s \right\}$$



4. A look at renormalization-group improved equation

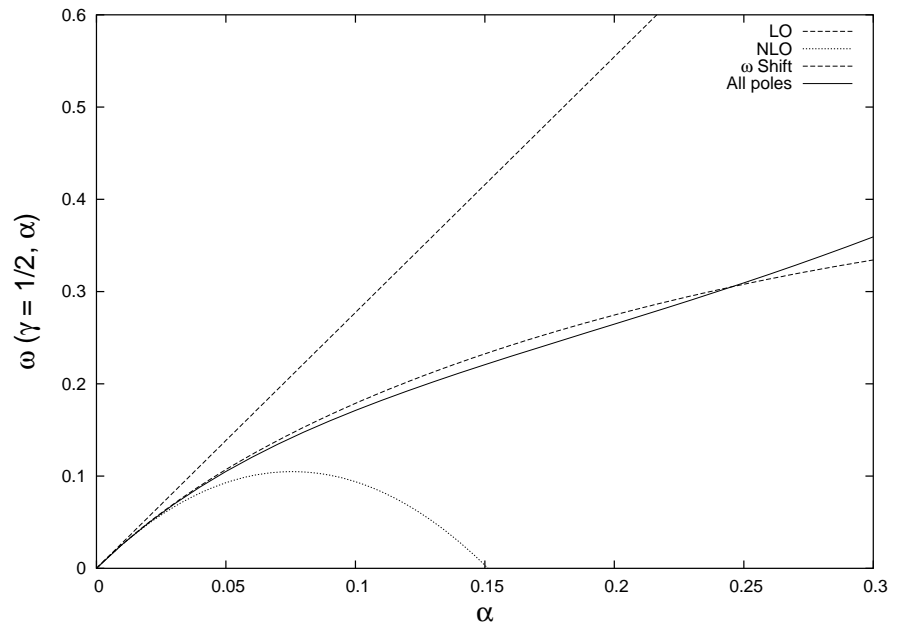
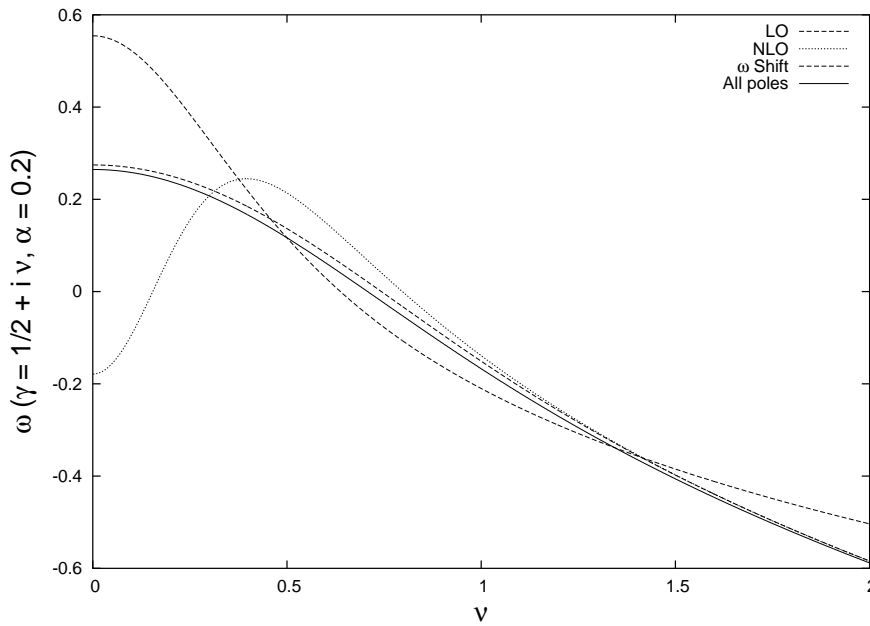
Including all terms and matching at NLL: No γ/ω mixing, $\omega = \omega(\gamma)$

$$\omega = \bar{\alpha}_s \chi_0(\gamma) + \bar{\alpha}_s^2 \chi_1(\gamma) + \sum_{m=0}^{\infty} \sum_{n=0}^{\infty} \frac{(-1)^n (2n)!}{2^n n! (n+1)!} \frac{(\bar{\alpha}_s + a \bar{\alpha}_s^2)^{n+1}}{(\gamma + m - b \bar{\alpha}_s)^{2n+1}} - M T$$



4. A look at renormalization-group improved equation

$$\omega = \bar{\alpha}_s \chi_0(\gamma) + \bar{\alpha}_s^2 \chi_1(\gamma) + \sum_{m=0}^{\infty} \sum_{n=0}^{\infty} \frac{(-1)^n (2n)!}{2^n n! (n+1)!} \frac{(\bar{\alpha}_s + a \bar{\alpha}_s^2)^{n+1}}{(\gamma + m - b \bar{\alpha}_s)^{2n+1}} - M T$$



4. A look at renormalization-group improved equation

Modification of original kernel is to remove the term $-\frac{\bar{\alpha}_s^2}{4} \frac{1}{(\mathbf{q}-\mathbf{k})^2} \ln^2 \left(\frac{q^2}{k^2} \right)$ in the real emission kernel, $\mathcal{K}_r(\mathbf{q}, \mathbf{k})$, and replace it with

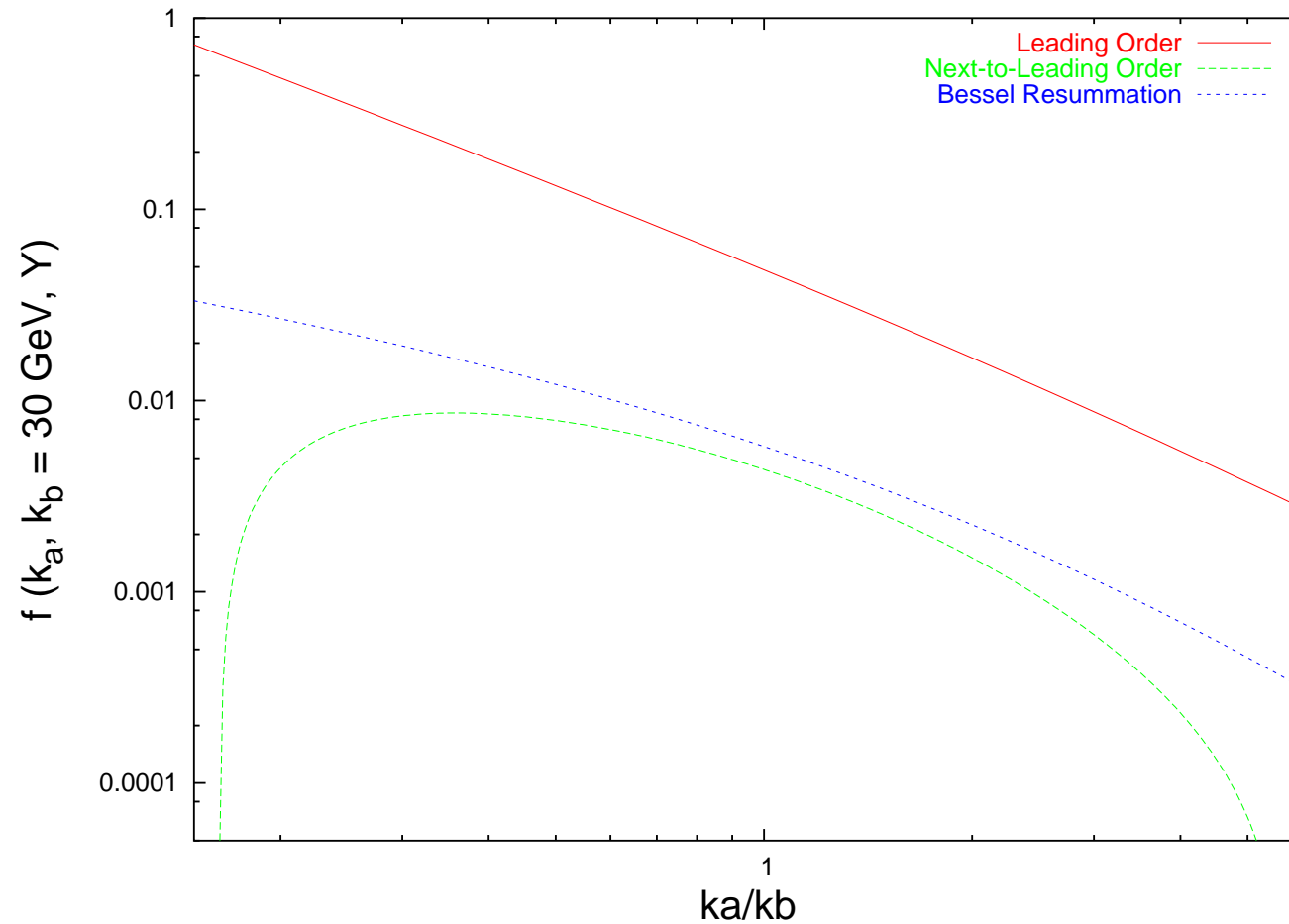
$$\frac{1}{(\mathbf{q}-\mathbf{k})^2} \left(\frac{q^2}{k^2} \right)^{-b\bar{\alpha}_s \frac{|k-q|}{k-q}} \sqrt{\frac{2(\bar{\alpha}_s + a\bar{\alpha}_s^2)}{\ln^2 \left(\frac{q^2}{k^2} \right)}} J_1 \left(\sqrt{2(\bar{\alpha}_s + a\bar{\alpha}_s^2) \ln^2 \left(\frac{q^2}{k^2} \right)} \right) - M T$$

$$J_1 \left(\sqrt{2\bar{\alpha}_s \ln^2 \left(\frac{q^2}{k^2} \right)} \right) \simeq \sqrt{\frac{\bar{\alpha}_s}{2} \ln^2 \left(\frac{q^2}{k^2} \right)}$$

$$J_1 \left(\sqrt{2\bar{\alpha}_s \ln^2 \left(\frac{q^2}{k^2} \right)} \right) \simeq \left(\frac{2}{\pi^2 \bar{\alpha}_s \ln^2 \left(\frac{q^2}{k^2} \right)} \right)^{\frac{1}{4}} \cos \left(\sqrt{2\bar{\alpha}_s \ln^2 \left(\frac{q^2}{k^2} \right)} - \frac{3\pi}{4} \right)$$

This generates a good collinear behaviour ...

4. A look at renormalization-group improved equation

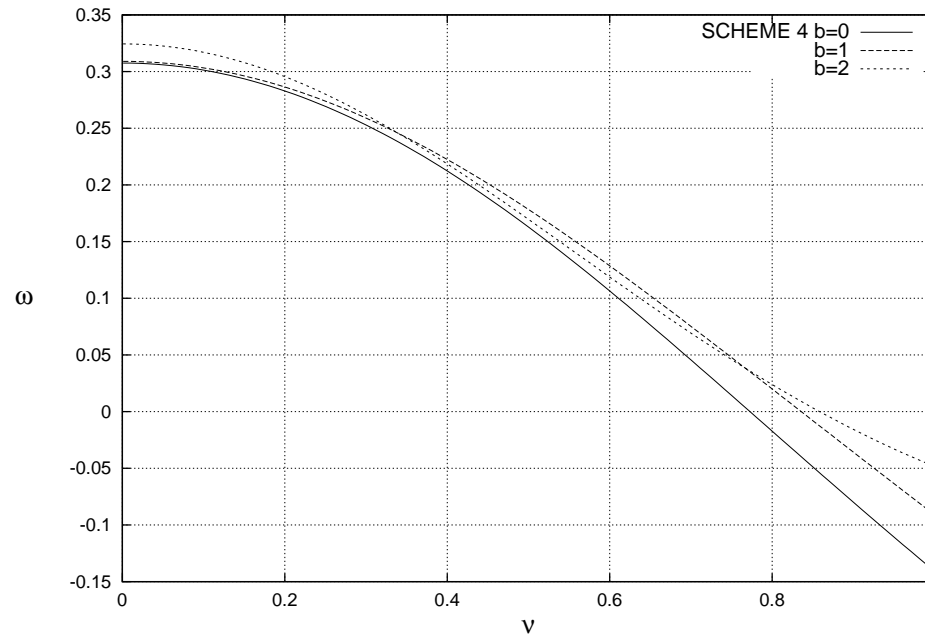


4. A look at renormalization-group improved equation

The effect of the rapidity veto and the collinear resummation is similar:

$$\omega = \bar{\alpha}_s e^{-b\omega} \left\{ (1 - \bar{\alpha}_s A)[2\psi(1) - \psi(\gamma + \omega/2 + \bar{\alpha}_s B') - \psi(1 - \gamma + \omega/2 + \bar{\alpha}_s B')] \right.$$

$$\left. + \bar{\alpha}_s \left[\chi_1(\gamma) + b\chi_0(\gamma)^2 + \left(\frac{1}{2}\chi_0(\gamma) + B' \right) (\psi'(\gamma) + \psi'(1 - \gamma)) + A\chi_0(\gamma) \right] \right\}$$

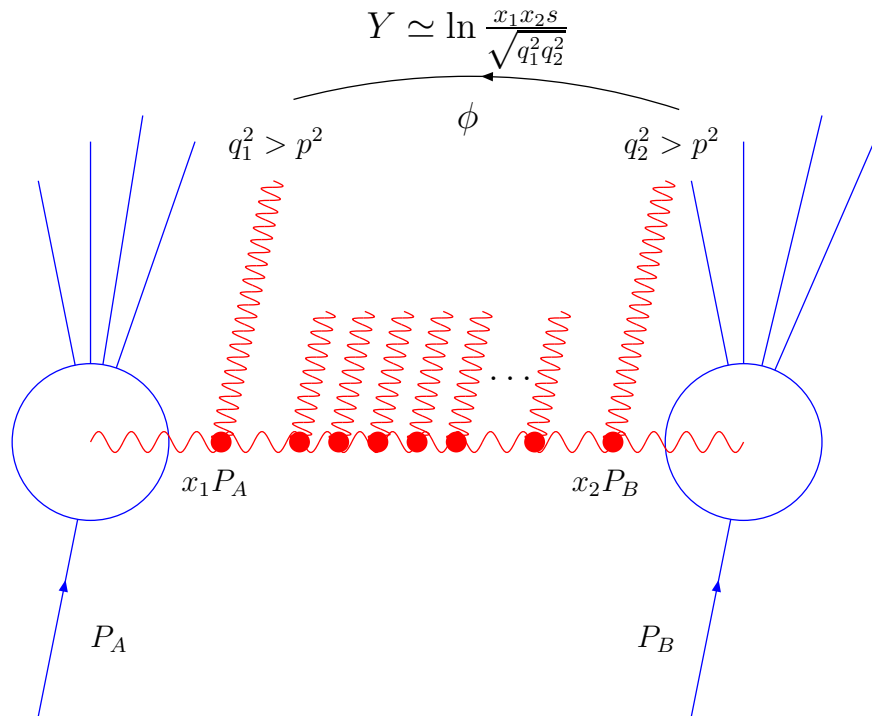




5. Azimuthal angles in Mueller–Navelet jets



5. Azimuthal angles in Mueller–Navelet jets



5. Azimuthal angles in Mueller–Navelet jets

$$\frac{d\hat{\sigma}}{d^2\vec{q}_1 d^2\vec{q}_2} = \frac{\pi^2 \bar{\alpha}_s^2}{2} \frac{f(\vec{q}_1, \vec{q}_2, Y)}{q_1^2 q_2^2}$$

The gluon Green's function

$$f(\vec{q}_1, \vec{q}_2, Y) = \int \frac{d\omega}{2\pi i} e^{\omega Y} f_\omega(\vec{q}_1, \vec{q}_2),$$

carries the dependence on Y .

$$\hat{q} |\vec{q}_i\rangle = \vec{q}_i |\vec{q}_i\rangle,$$

with normalization

$$\langle \vec{q}_1 | \hat{1} | \vec{q}_2 \rangle = \delta^{(2)}(\vec{q}_1 - \vec{q}_2),$$

can be written as

$$(\omega - \bar{\alpha}_s \hat{K}_0 - \bar{\alpha}_s^2 \hat{K}_1) \hat{f}_\omega = \hat{1}.$$

5. Azimuthal angles in Mueller–Navelet jets

Basis: $\langle \vec{q} | \nu, n \rangle = \frac{1}{\pi\sqrt{2}} (q^2)^{i\nu - \frac{1}{2}} e^{in\theta}$.

As Y increases the azimuthal angle dependence is driven by the kernel. This is the reason why we use the LO jet vertices which are much simpler than the NLO. The differential cross section in the azimuthal angle $\phi = \theta_1 - \theta_2 - \pi$, where θ_i are the angles of the two tagged jets, is

$$\frac{d\hat{\sigma}(\alpha_s, Y, p_{1,2}^2)}{d\phi} = \frac{\pi^2 \bar{\alpha}_s^2}{4\sqrt{p_1^2 p_2^2}} \sum_{n=-\infty}^{\infty} e^{in\phi} \mathcal{C}_n(Y),$$

with

$$\mathcal{C}_n(Y) = \frac{1}{2\pi} \int_{-\infty}^{\infty} \frac{d\nu}{\left(\frac{1}{4} + \nu^2\right)} \left(\frac{p_1^2}{p_2^2}\right)^{i\nu} e^{\chi(|n|, \frac{1}{2} + i\nu, \bar{\alpha}_s(p_1 p_2))Y},$$

and

$$\chi(n, \gamma, \bar{\alpha}_s) \equiv \bar{\alpha}_s \chi_0(n, \gamma) + \bar{\alpha}_s^2 \left(\chi_1(n, \gamma) - \frac{\beta_0}{8N_c} \frac{\chi_0(n, \gamma)}{\gamma(1-\gamma)} \right).$$

5. Azimuthal angles in Mueller–Navelet jets

\mathcal{C}_n are not evaluated at the saddle point, but obtained by a numerical integration over the full range of ν . The LO kernel, \hat{K}_0 , has eigenvalue

$$\chi_0(n, \gamma) = 2\psi(1) - \psi\left(\gamma + \frac{n}{2}\right) - \psi\left(1 - \gamma + \frac{n}{2}\right),$$

The eigenvalue of the scale invariant NLO sector is

$$\begin{aligned} \chi_1(n, \gamma) &= \mathcal{S}\chi_0(n, \gamma) + \frac{3}{2}\zeta(3) - \frac{\beta_0}{8N_c}\chi_0^2(n, \gamma) \\ &+ \frac{1}{4}\left[\psi''\left(\gamma + \frac{n}{2}\right) + \psi''\left(1 - \gamma + \frac{n}{2}\right) - 2\phi(n, \gamma) - 2\phi(n, 1 - \gamma)\right] \\ &- \frac{\pi^2 \cos(\pi\gamma)}{4\sin^2(\pi\gamma)(1 - 2\gamma)} \left\{ \left[3 + \left(1 + \frac{n_f}{N_c^3}\right) \frac{2 + 3\gamma(1 - \gamma)}{(3 - 2\gamma)(1 + 2\gamma)}\right] \delta_n^0 \right. \\ &\quad \left. - \left(1 + \frac{n_f}{N_c^3}\right) \frac{\gamma(1 - \gamma)}{2(3 - 2\gamma)(1 + 2\gamma)} \delta_n^2 \right\}, \end{aligned}$$

The full cross section corresponds to the integration over the azimuthal angle and it only depends on the $n = 0$ component:

$$\hat{\sigma} (\alpha_s, Y, p_{1,2}^2) = \frac{\pi^3 \bar{\alpha}_s^2}{2\sqrt{p_1^2 p_2^2}} \mathcal{C}_0 (Y).$$

We are interested in distributions sensitive to higher conformal spins. The average of the cosine of the azimuthal angle times an integer projects out the contribution from each of these angular components::

$$\langle \cos(m\phi) \rangle = \frac{\mathcal{C}_m(Y)}{\mathcal{C}_0(Y)}.$$

The associated ratios

$$\frac{\langle \cos(m\phi) \rangle}{\langle \cos(n\phi) \rangle} = \frac{\mathcal{C}_m(Y)}{\mathcal{C}_n(Y)}$$

can be used to remove the uncertainty associated to the $n = 0$ component.

All angular components together are present in the normalized differential cross section:

$$\frac{1}{\hat{\sigma}} \frac{d\hat{\sigma}}{d\phi} = \frac{1}{2\pi} \sum_{n=-\infty}^{\infty} e^{in\phi} \frac{\mathcal{C}_n(Y)}{\mathcal{C}_0(Y)} = \frac{1}{2\pi} \left\{ 1 + 2 \sum_{n=1}^{\infty} \cos(n\phi) \langle \cos(n\phi) \rangle \right\}.$$

As we have seen before the BFKL resummation presents an instability at NLO. Our observables are very dependent on the renormalization scheme. The term proportional to χ_0 in χ_1 can be removed by a shift:

$$\Lambda_{\overline{\text{MS}}} \rightarrow \Lambda_{\text{GB}} = \Lambda_{\overline{\text{MS}}} e^{\frac{2N_c}{\beta_0} S}.$$

Convergence can be improved demanding compatibility with renormalization group evolution to all orders in the DIS limit, introducing a shift in the anomalous dimension. So far these types of resummations have been performed for a BFKL kernel averaged over the azimuthal angle and only affect the zero conformal spin. We now study the convergence of the eigenvalues for all angular components.

5. Azimuthal angles in Mueller–Navelet jets

First we extract the poles at $\gamma = -\frac{n}{2}, 1 + \frac{n}{2}$:

$$\begin{aligned}
 \chi_0(n, \gamma) &\simeq \frac{1}{\gamma + \frac{n}{2}} + \{\gamma \rightarrow 1 - \gamma\}, \\
 \chi_1(n, \gamma) &\simeq \frac{a_n}{\gamma + \frac{n}{2}} + \frac{b_n}{(\gamma + \frac{n}{2})^2} - \frac{1}{2(\gamma + \frac{n}{2})^3} + \frac{c\delta_n^2}{\gamma} + \{\gamma \rightarrow 1 - \gamma\}. \\
 a_n &= \mathcal{S} - \frac{\pi^2}{24} + \frac{\beta_0}{4N_c} H_n + \frac{1}{8} \left(\psi' \left(\frac{n+1}{2} \right) - \psi' \left(\frac{n+2}{2} \right) \right) + \frac{1}{2} \psi'(n+1) \\
 &\quad - \frac{\delta_n^0}{36} \left(67 + 13 \frac{n_f}{N_c^3} \right) - \frac{47\delta_n^2}{1800} \left(1 + \frac{n_f}{N_c^3} \right), \\
 -b_n &= \frac{\beta_0}{8N_c} + \frac{1}{2} H_n + \frac{\delta_n^0}{12} \left(11 + 2 \frac{n_f}{N_c^3} \right) + \frac{\delta_n^2}{60} \left(1 + \frac{n_f}{N_c^3} \right), \\
 c &= \frac{1}{24} \left(1 + \frac{n_f}{N_c^3} \right).
 \end{aligned}$$

Here H_n stands for the harmonic number $\psi(n+1) - \psi(1)$.

5. Azimuthal angles in Mueller–Navelet jets

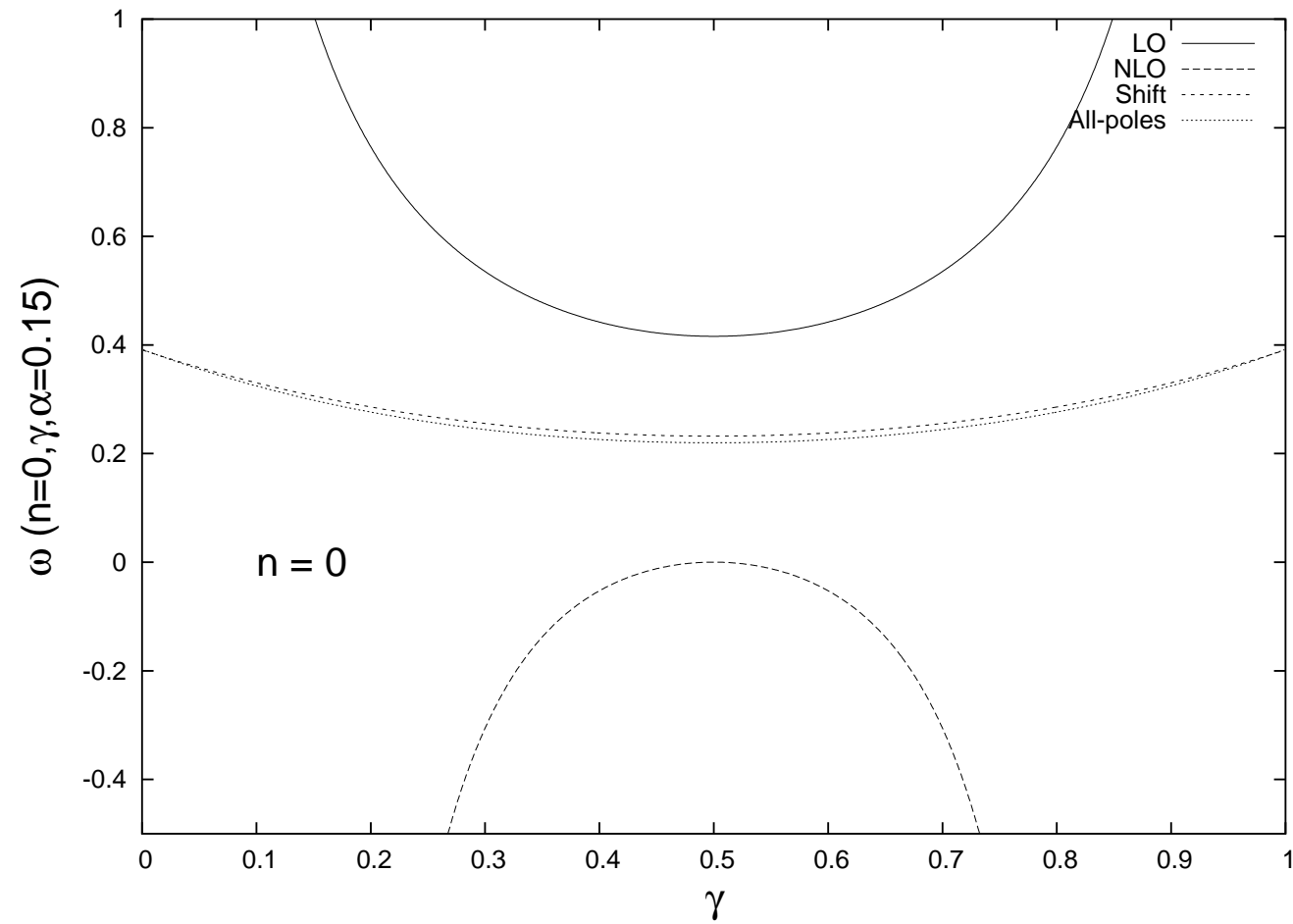
We use the resummation scheme:

$$\begin{aligned} \omega = & \bar{\alpha}_s (1 + \mathcal{A}_n \bar{\alpha}_s) \left\{ 2 \psi(1) - \psi \left(\gamma + \frac{|n|}{2} + \frac{\omega}{2} + \mathcal{B}_n \bar{\alpha}_s \right) \right. \\ & \left. - \psi \left(1 - \gamma + \frac{|n|}{2} + \frac{\omega}{2} + \mathcal{B}_n \bar{\alpha}_s \right) \right\} + \bar{\alpha}_s^2 \left\{ \chi_1(|n|, \gamma) - \frac{\beta_0}{8N_c} \frac{\chi_0(n, \gamma)}{\gamma(1-\gamma)} \right. \\ & \left. - \mathcal{A}_n \chi_0(|n|, \gamma) \right\} + \left(\psi' \left(\gamma + \frac{|n|}{2} \right) + \psi' \left(1 - \gamma + \frac{|n|}{2} \right) \right) \left(\frac{\chi_0(|n|, \gamma)}{2} + \mathcal{B}_n \right) \end{aligned}$$

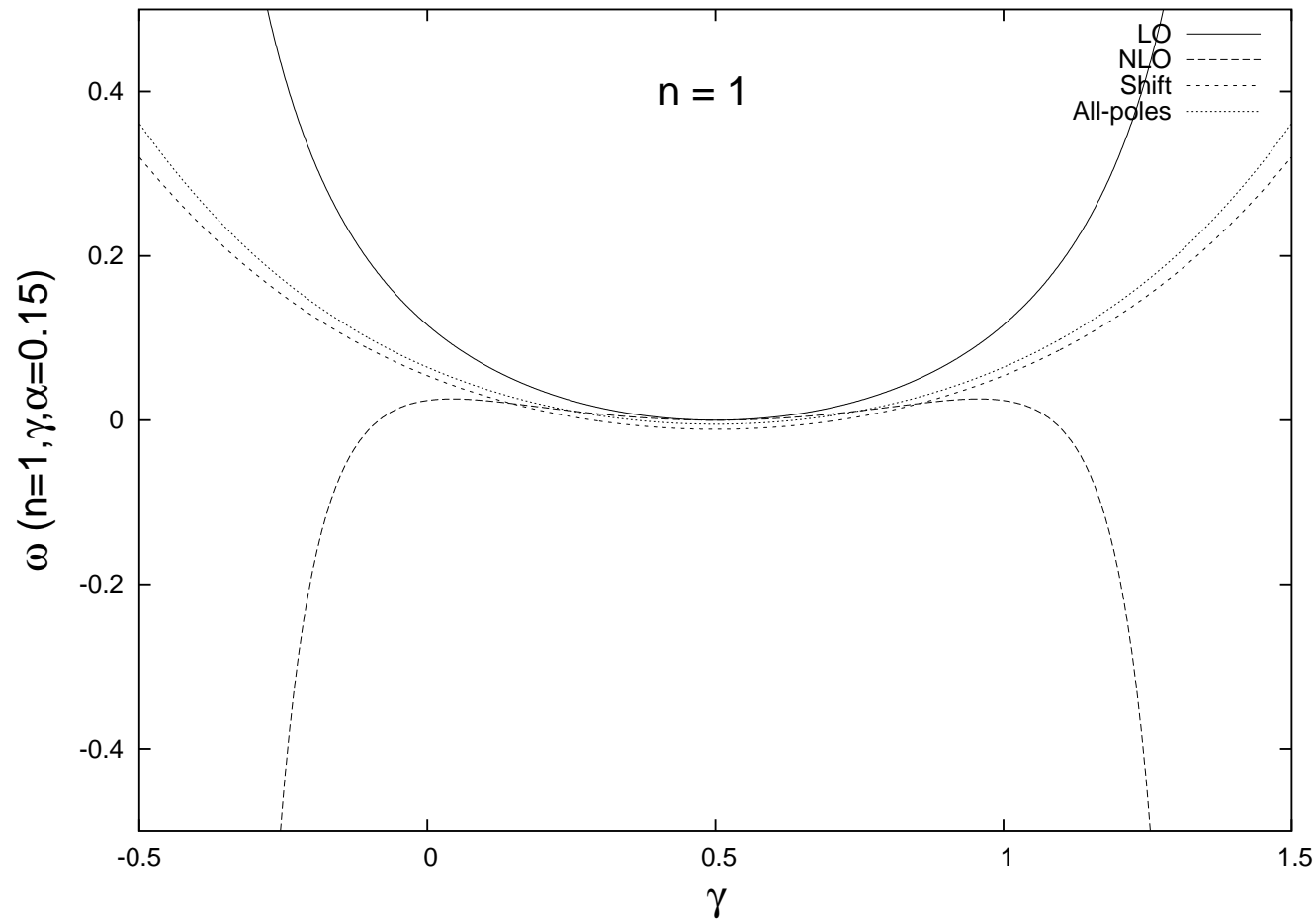
$$\mathcal{A}_n = a_n + \psi'(n+1),$$

$$\mathcal{B}_n = \frac{1}{2} H_n - b_n.$$

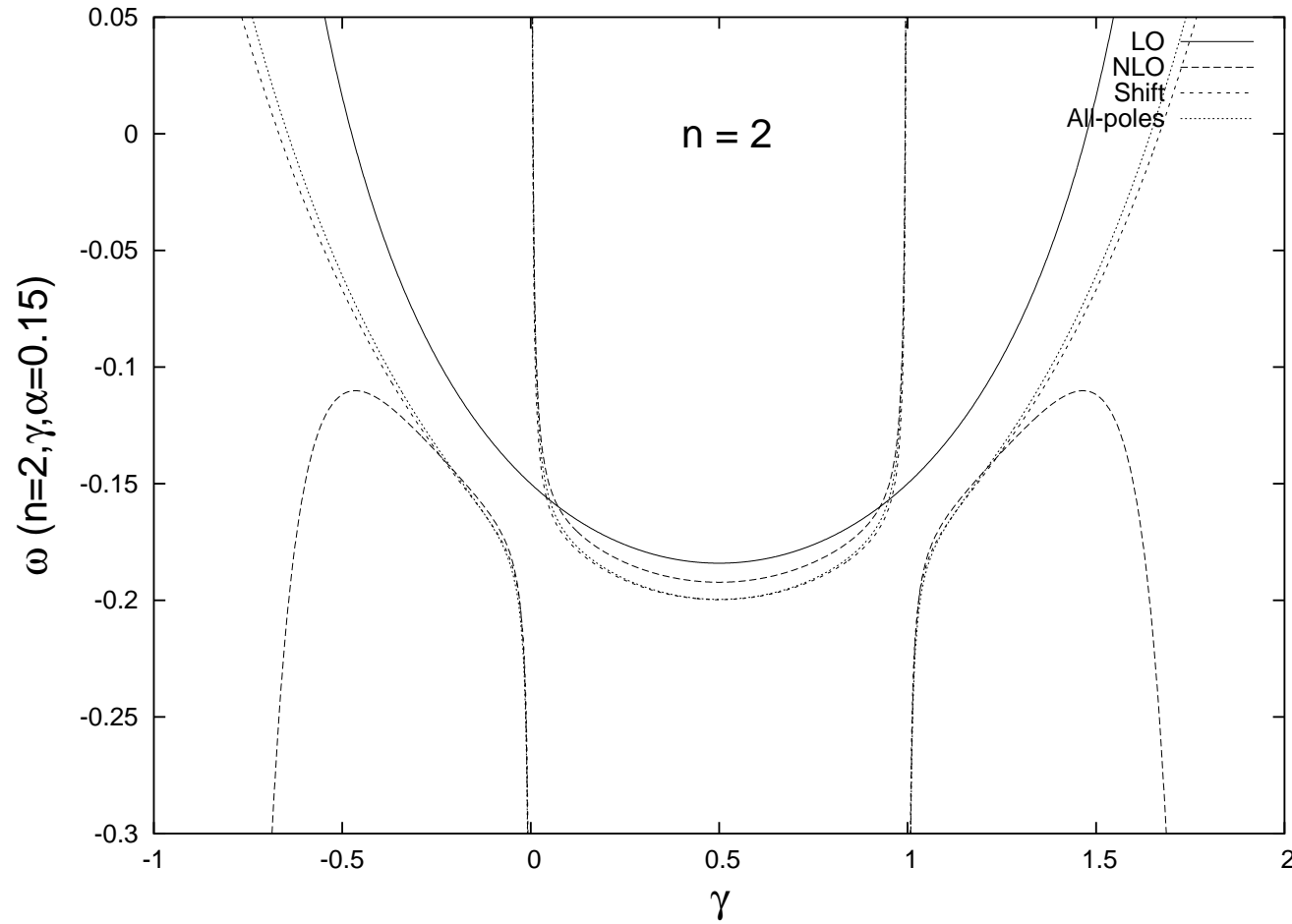
5. Azimuthal angles in Mueller–Navelet jets



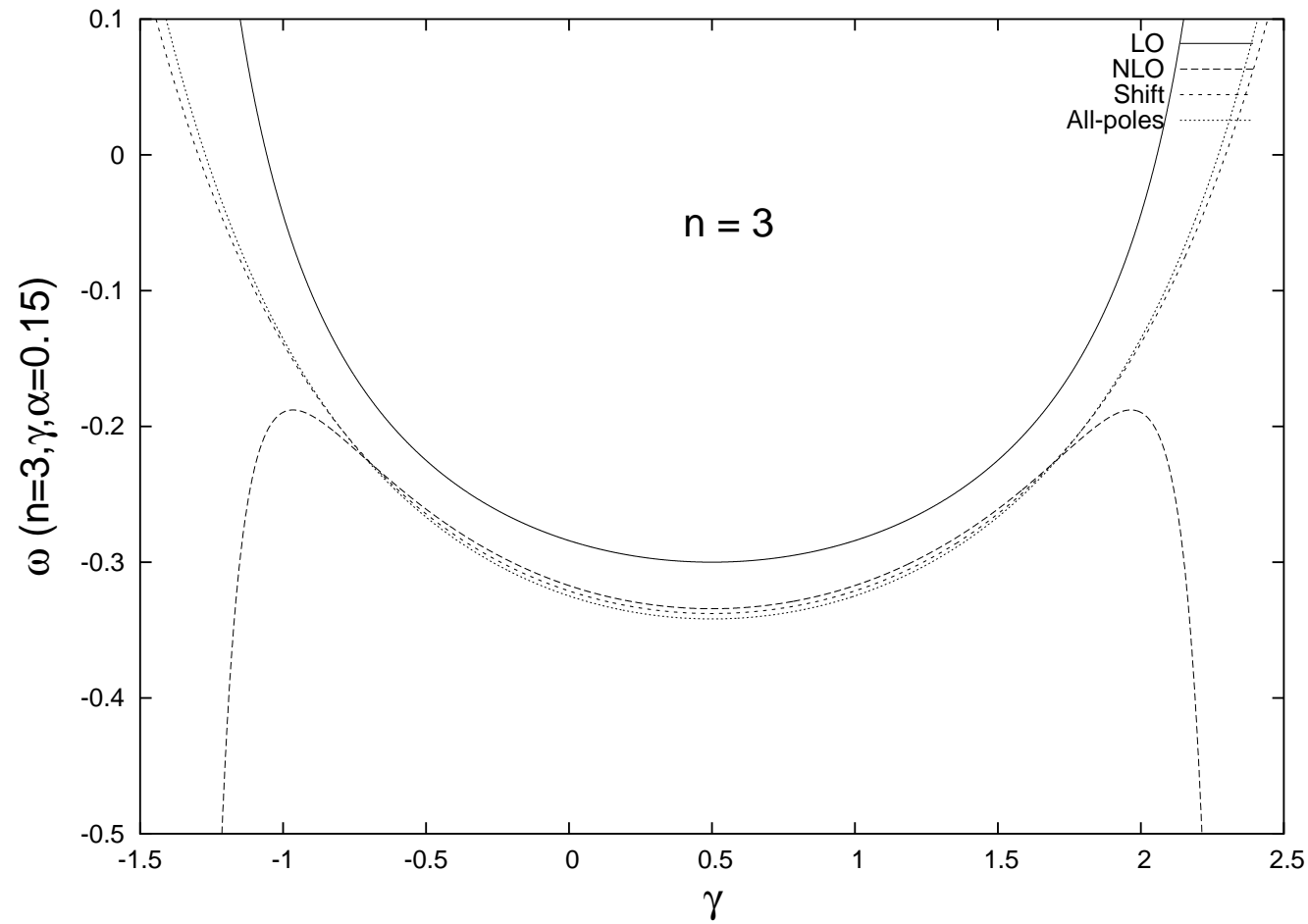
5. Azimuthal angles in Mueller–Navelet jets



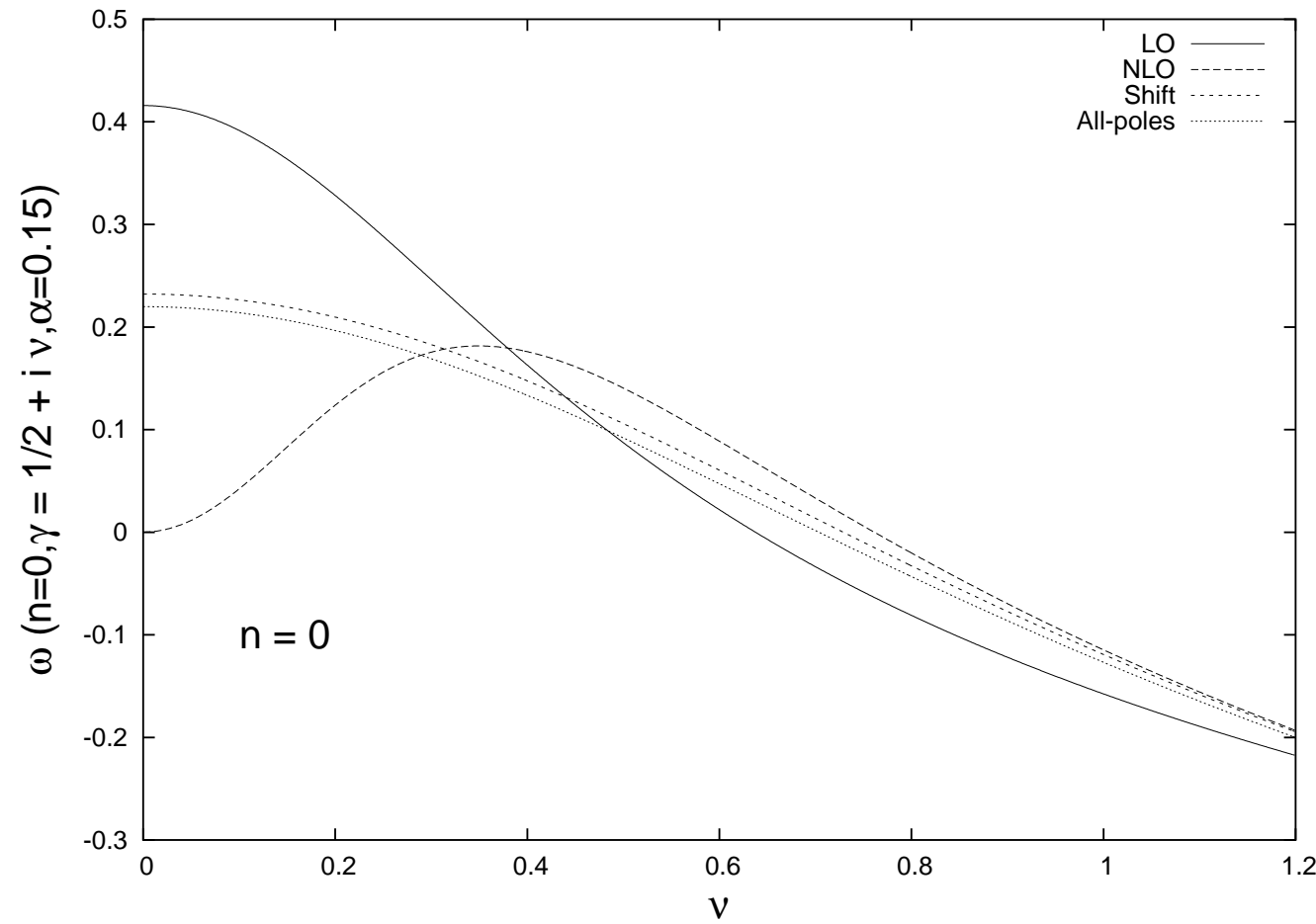
5. Azimuthal angles in Mueller–Navelet jets



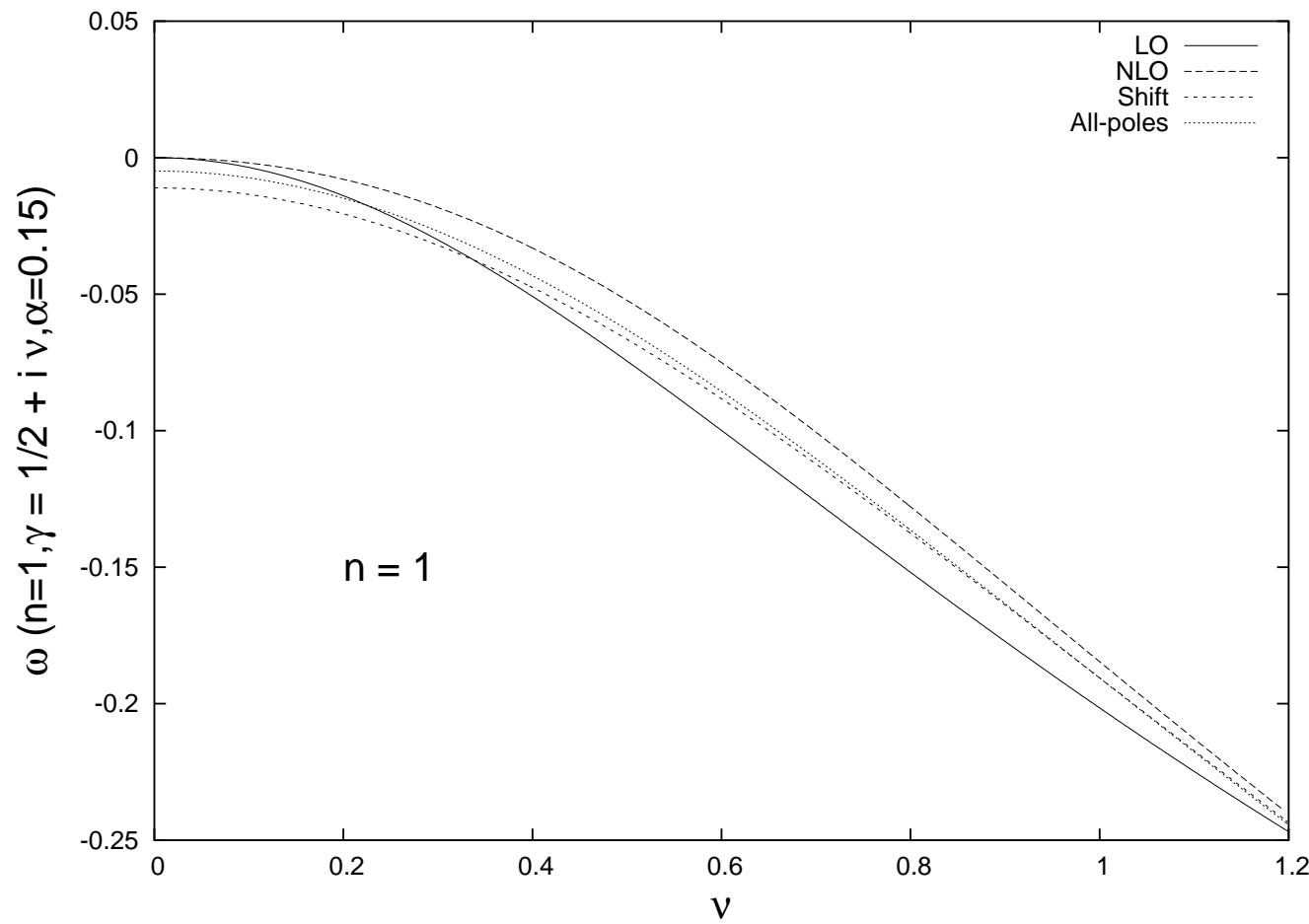
5. Azimuthal angles in Mueller–Navelet jets



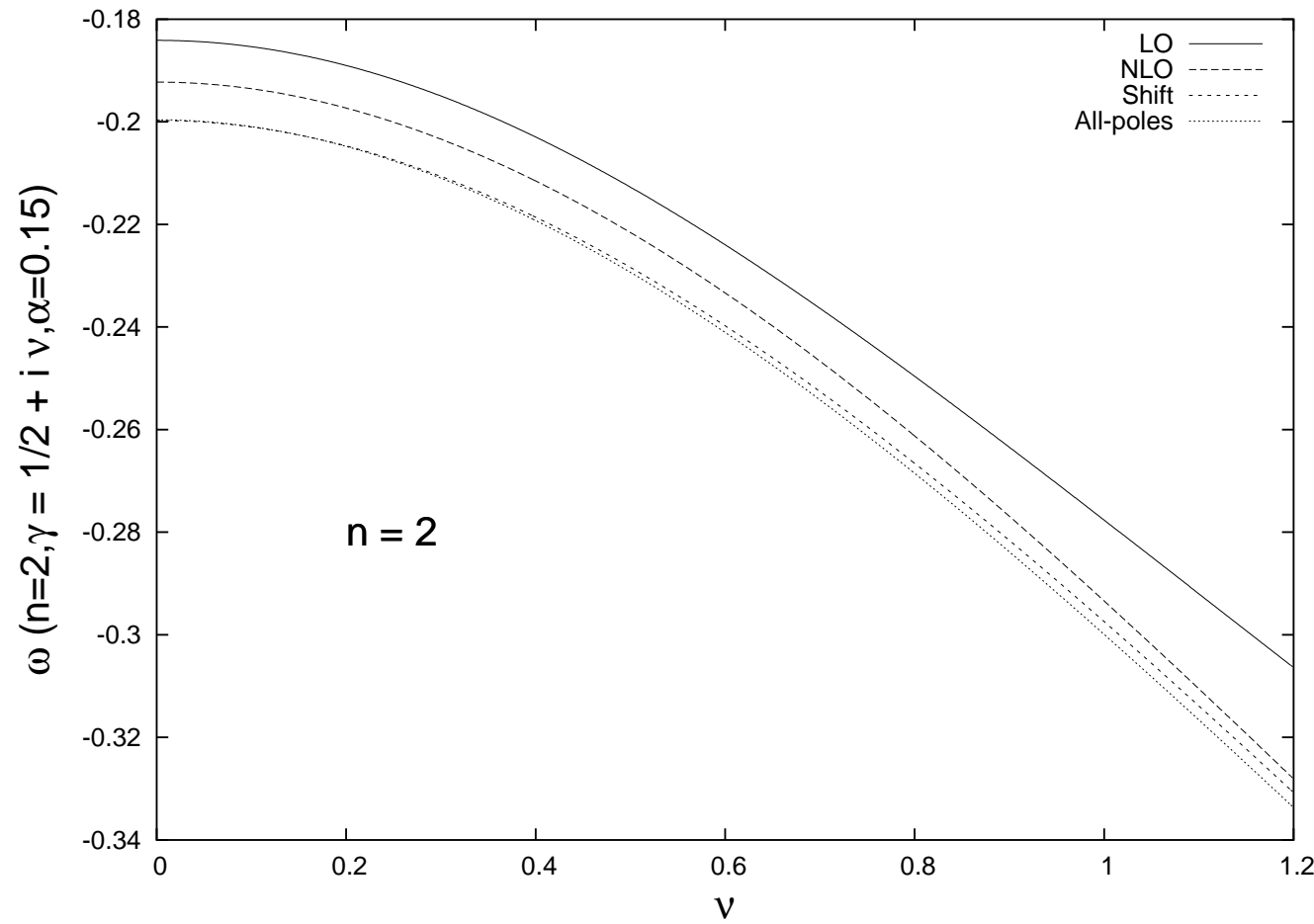
5. Azimuthal angles in Mueller–Navelet jets



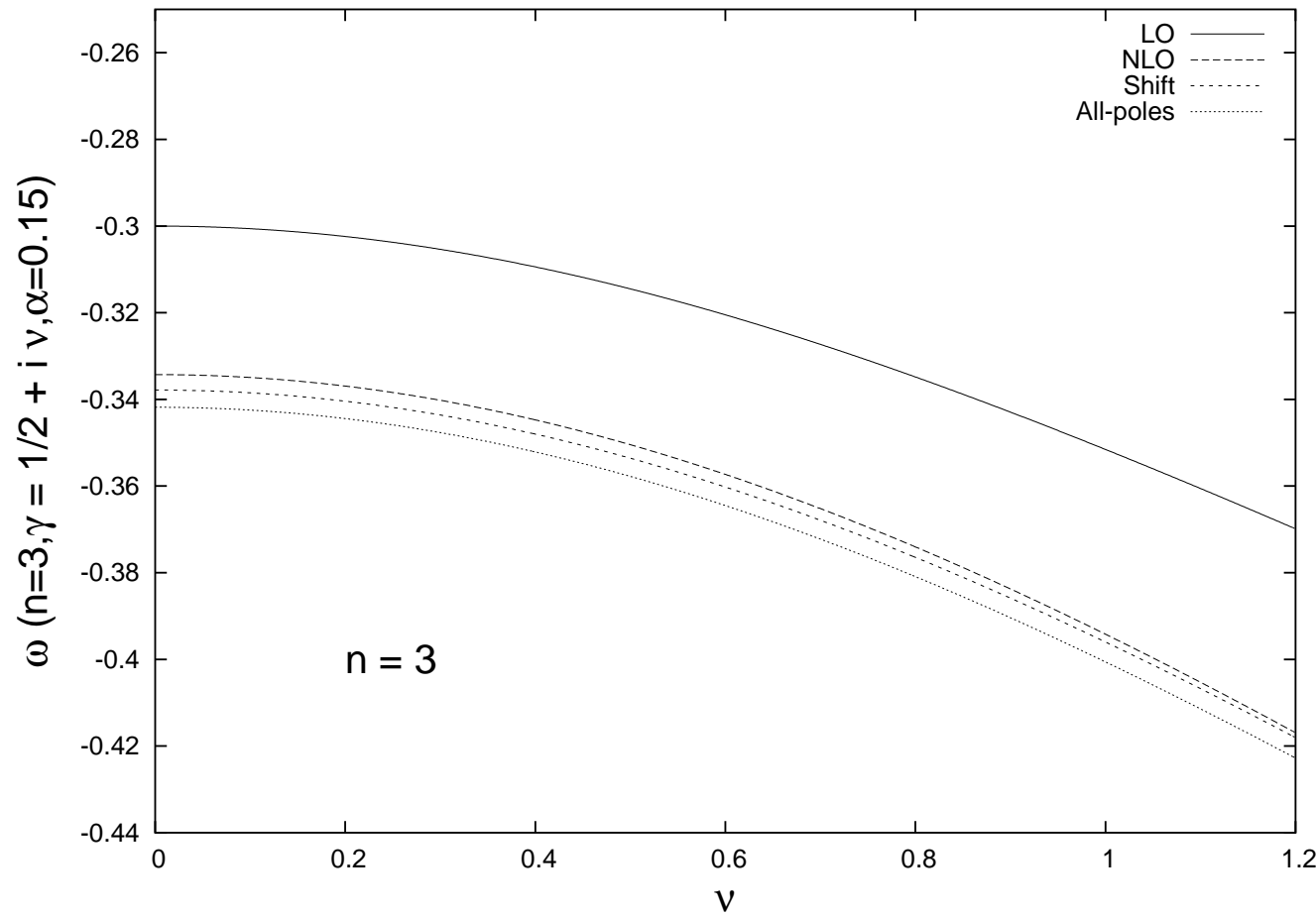
5. Azimuthal angles in Mueller–Navelet jets



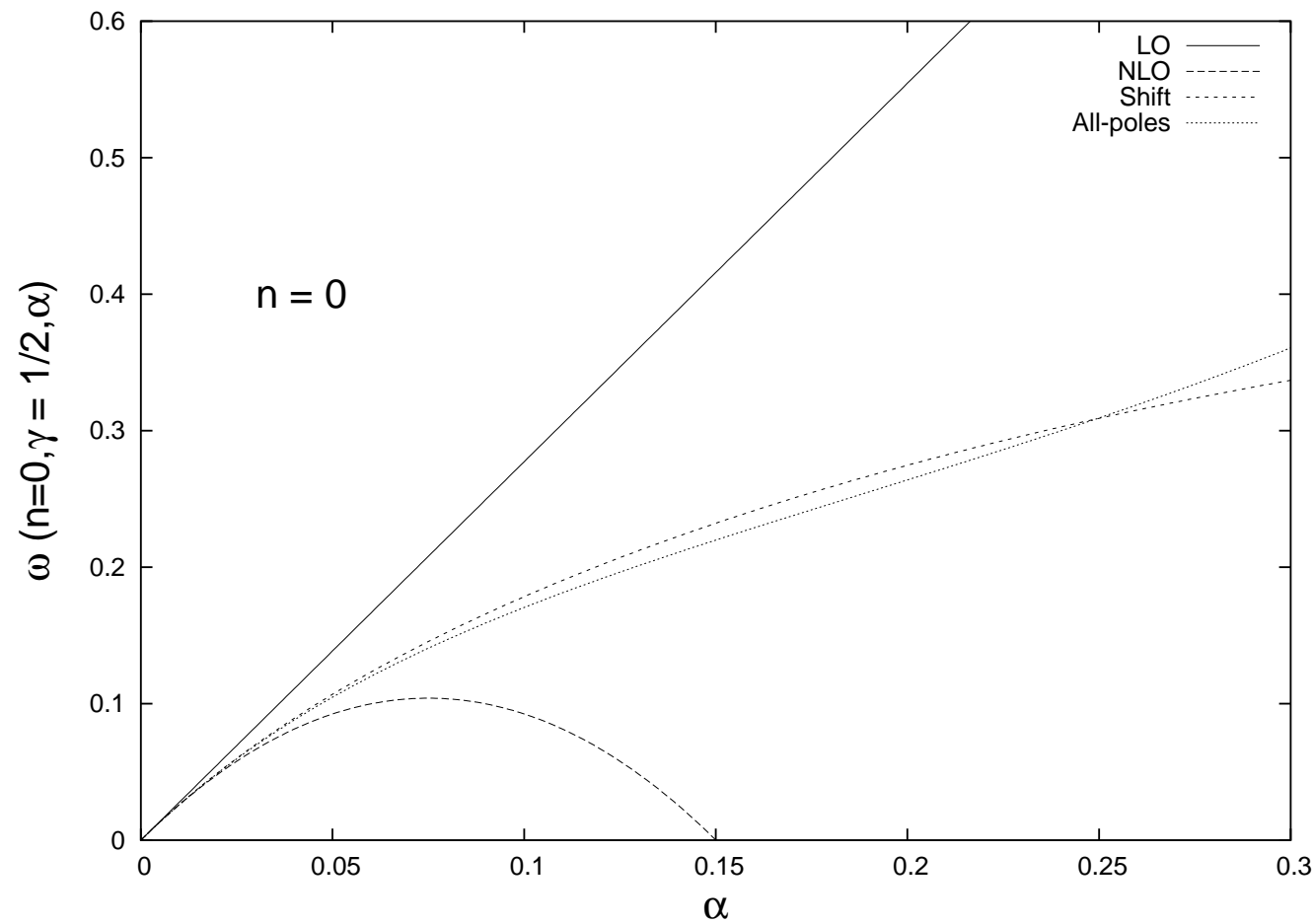
5. Azimuthal angles in Mueller–Navelet jets



5. Azimuthal angles in Mueller–Navelet jets



5. Azimuthal angles in Mueller–Navelet jets



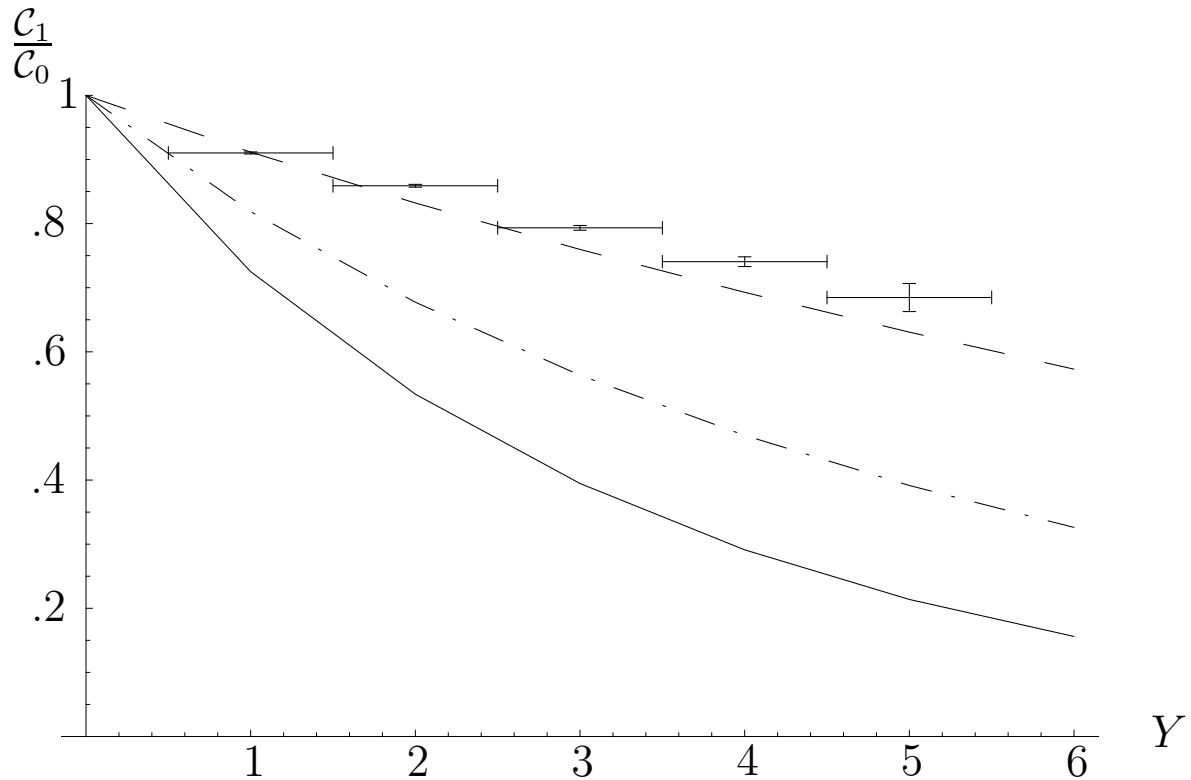
5. Azimuthal angles in Mueller–Navelet jets

Mueller and Navelet proposed this process as ideal to apply the BFKL formalism and predicted a power-like rise for the cross section. However, to realize this growth as a manifestation of multi–Regge kinematics is very difficult since it is drastically damped by the behaviour of the parton distribution functions for $x \rightarrow 1$.

The D \emptyset collaboration analyzed data taken at the Tevatron $p\bar{p}$ –collider from two periods of measurement at different energies $\sqrt{s} = 630$ and 1800 GeV. From these they extracted an intercept of $1.65 \pm .07$. This rise is even faster than that predicted in the LO BFKL calculation which for the kinematics relevant in the D \emptyset experiment yields an approximated value of 1.45.

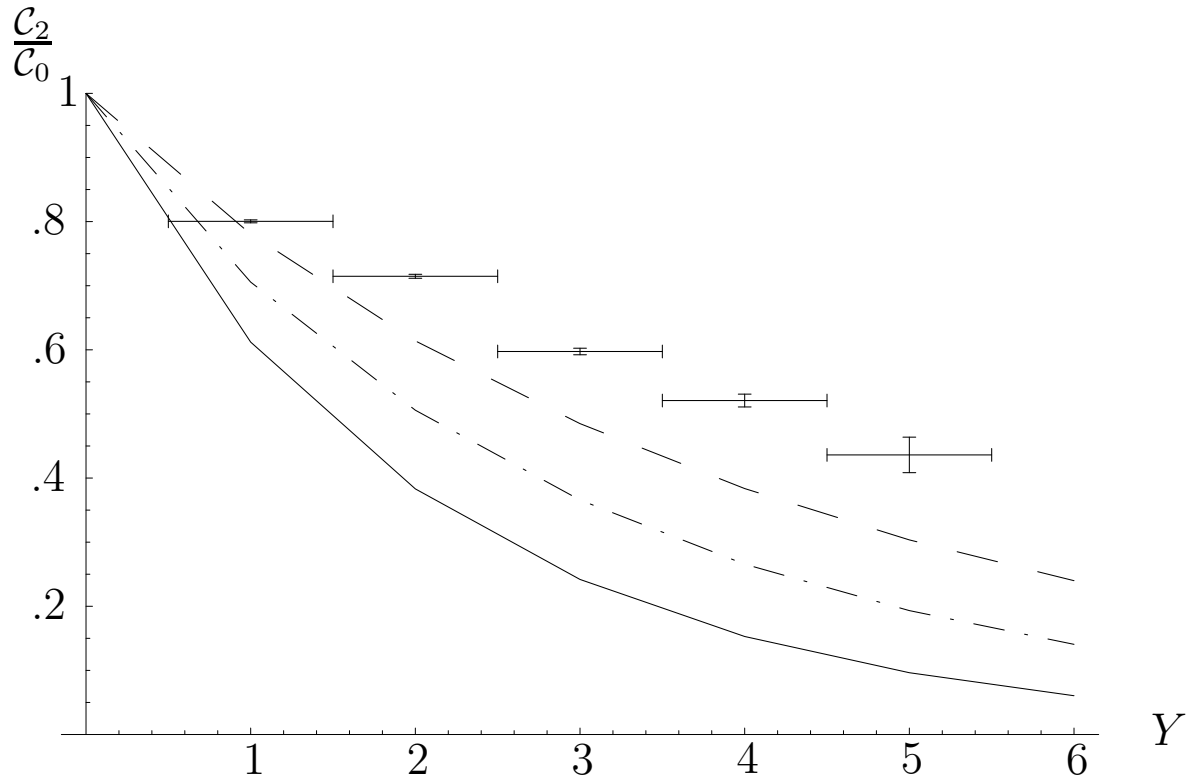
It is safer to study quantities insensitive to the pdf's ...

5. Azimuthal angles in Mueller–Navelet jets



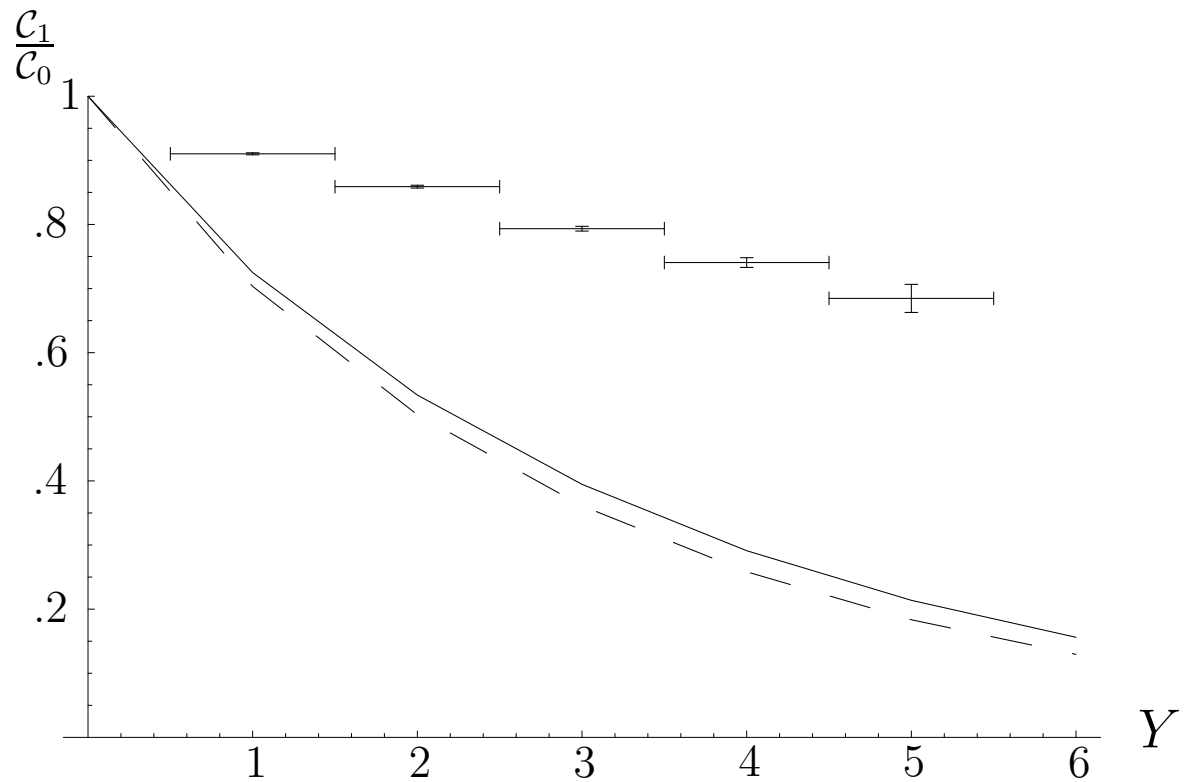
$\langle \cos \phi \rangle = C_1/C_0$ at a $p\bar{p}$ collider with $\sqrt{s} = 1.8$ TeV for BFKL at LO (solid) and NLO (dashed). The results from the resummation presented in the text are shown as well (dash-dotted).

5. Azimuthal angles in Mueller–Navelet jets



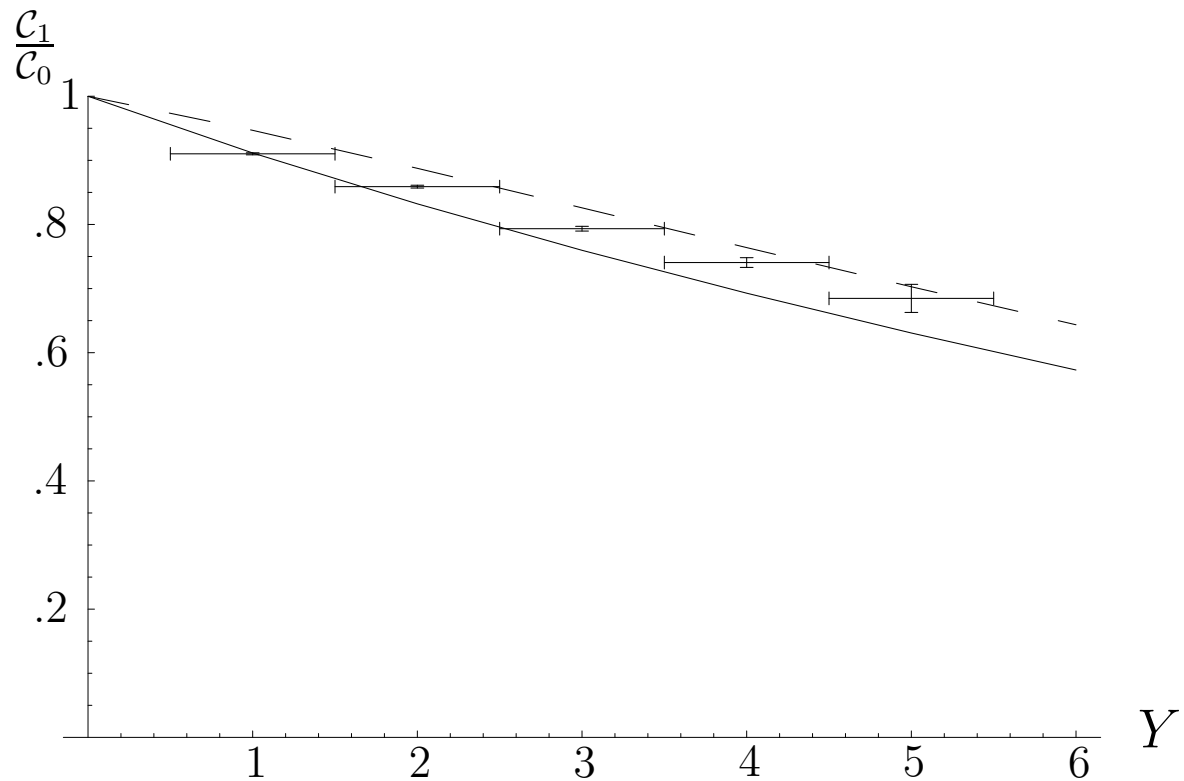
$\langle \cos 2\phi \rangle = C_2/C_0$ at a $p\bar{p}$ collider with $\sqrt{s} = 1.8$ TeV for BFKL at LO (solid) and NLO (dashed). The results from the resummation presented in the text are shown as well (dash-dotted).

5. Azimuthal angles in Mueller–Navelet jets



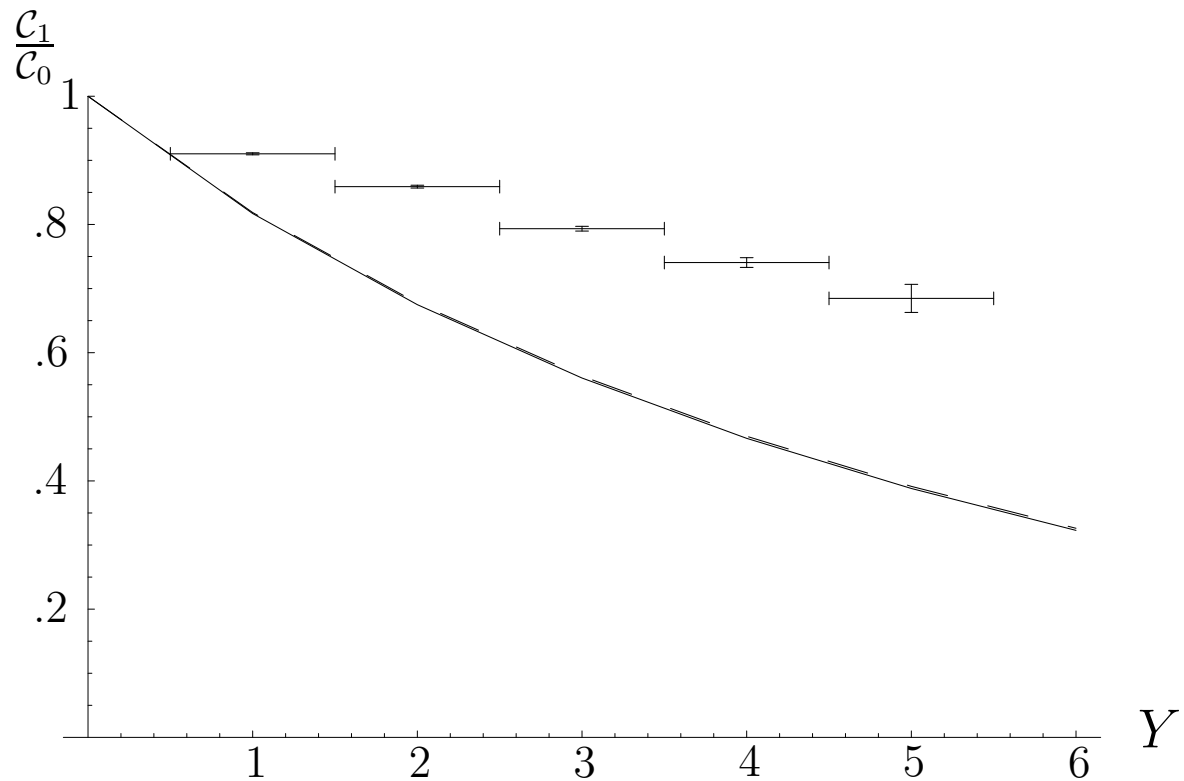
$\langle \cos \phi \rangle$ at LO comparing the $\overline{\text{MS}}$ renormalization scheme (solid) with the GB scheme (dashed).

5. Azimuthal angles in Mueller–Navelet jets



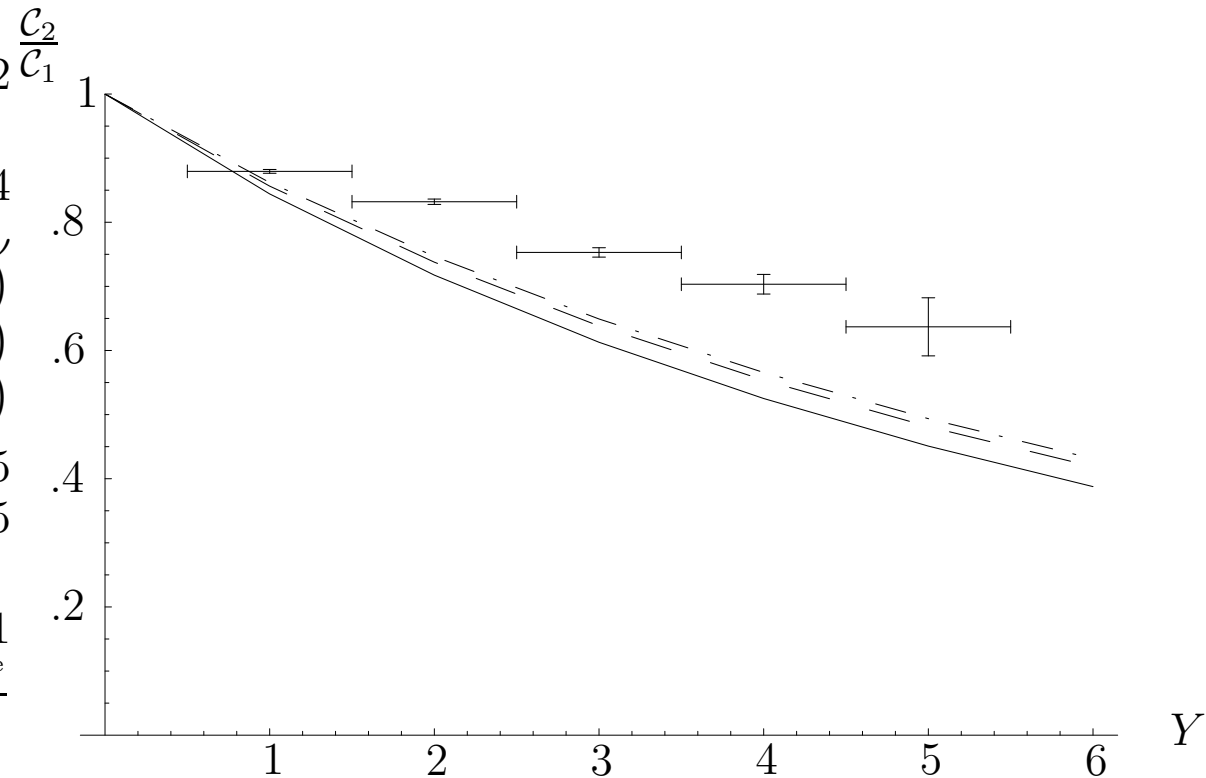
$\langle \cos \phi \rangle$ at NLO comparing the $\overline{\text{MS}}$ renormalization scheme (solid) with the GB scheme (dashed).

5. Azimuthal angles in Mueller–Navelet jets



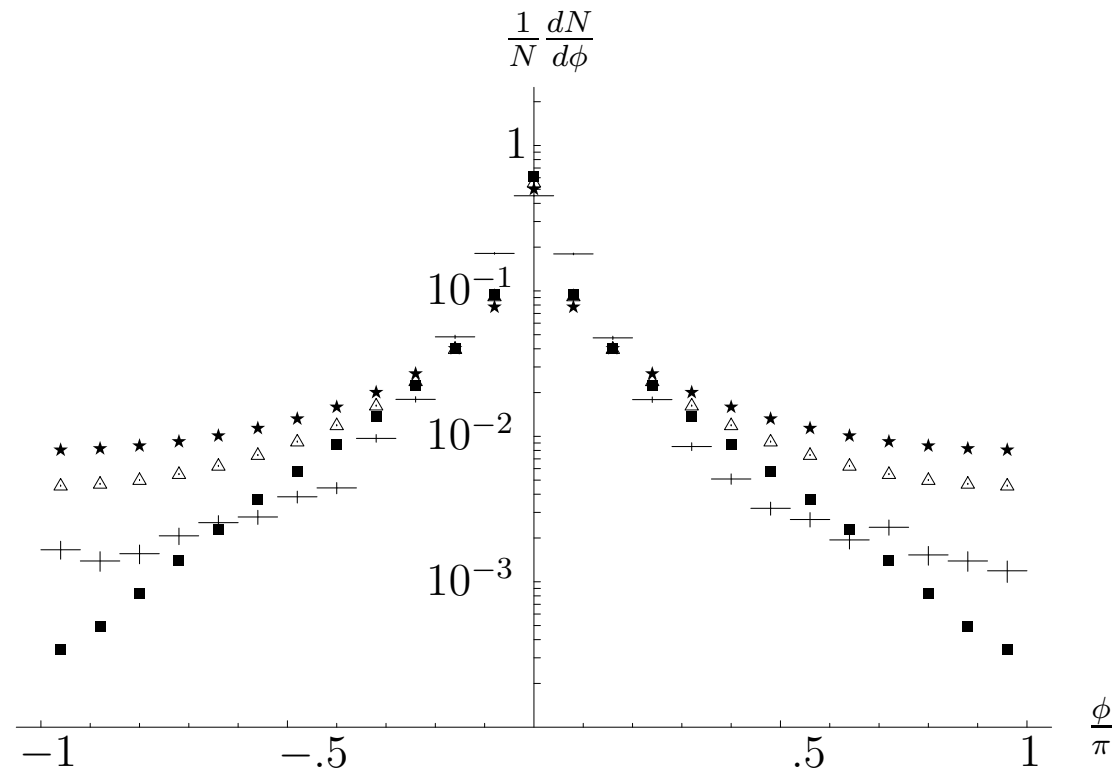
$\langle \cos \phi \rangle$ with a resummed kernel comparing the $\overline{\text{MS}}$ renormalization scheme (solid) with the GB scheme (dashed).

5. Azimuthal angles in Mueller–Navelet jets



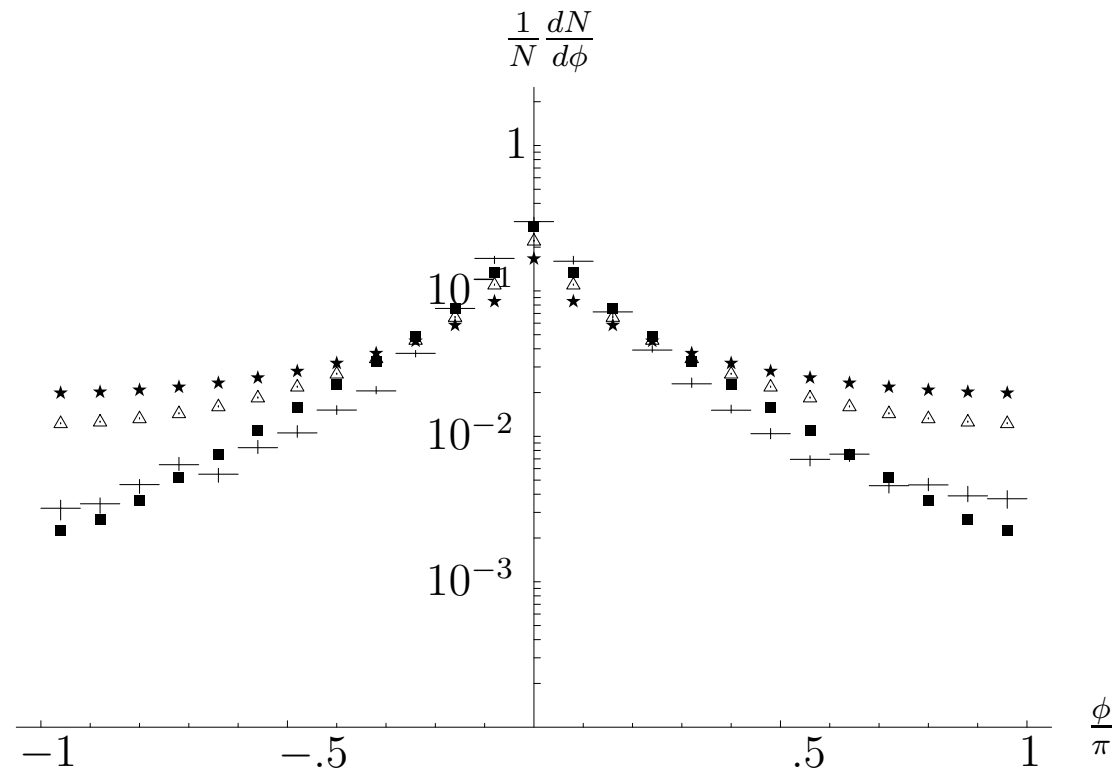
$\frac{\langle \cos 2\phi \rangle}{\langle \cos \phi \rangle} = \frac{C_2}{C_1}$ with LO (solid), NLO (dashed) and collinearly resummed (dash-dotted) BFKL kernels.

5. Azimuthal angles in Mueller–Navelet jets



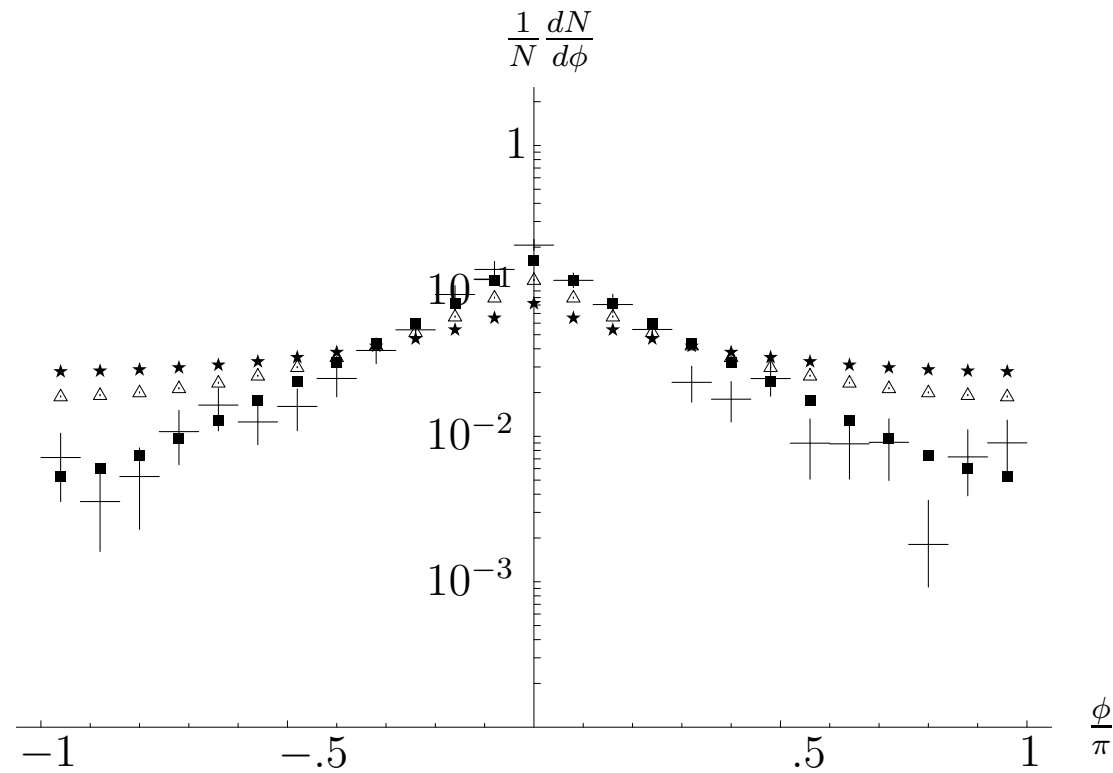
$\frac{1}{N} \frac{dN}{d\phi}$ in a $p\bar{p}$ collider at $\sqrt{s}=1.8$ TeV using a LO (stars), NLO (squares) and resummed (triangles) BFKL kernel. This plot is for $Y = 1$.

5. Azimuthal angles in Mueller–Navelet jets



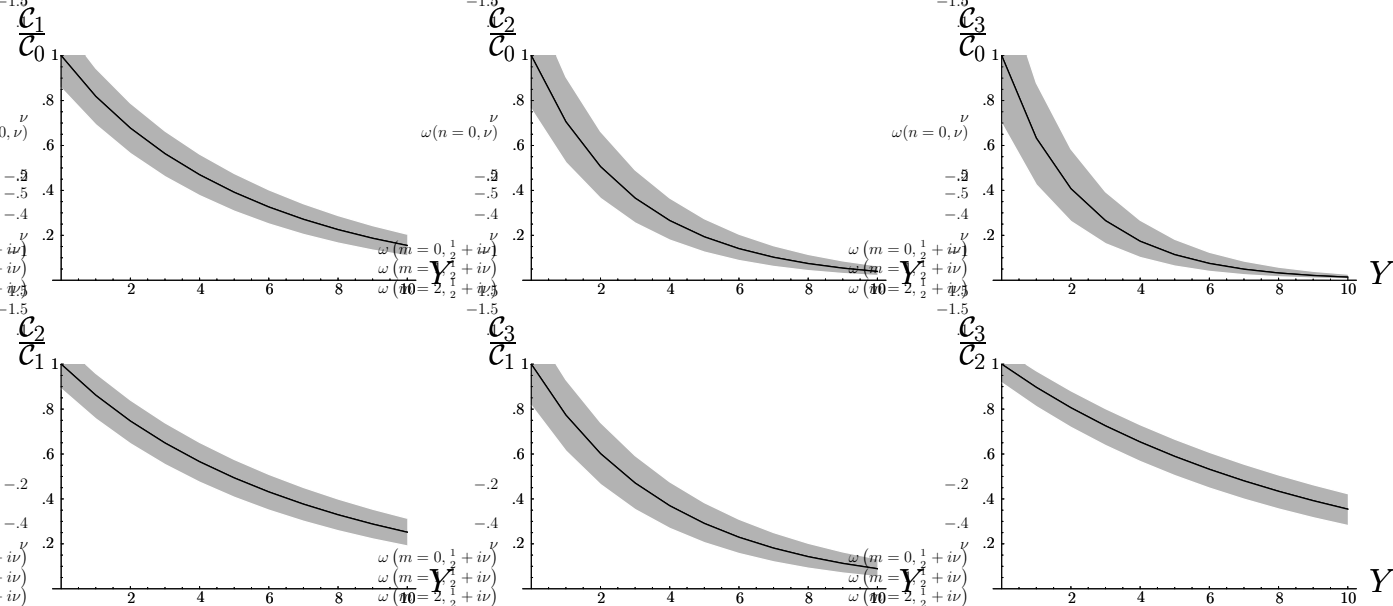
$\frac{1}{N} \frac{dN}{d\phi}$ in a $p\bar{p}$ collider at $\sqrt{s}=1.8$ TeV using a LO (stars), NLO (squares) and resummed (triangles) BFKL kernel. This plot is for $Y = 3$.

5. Azimuthal angles in Mueller–Navelet jets



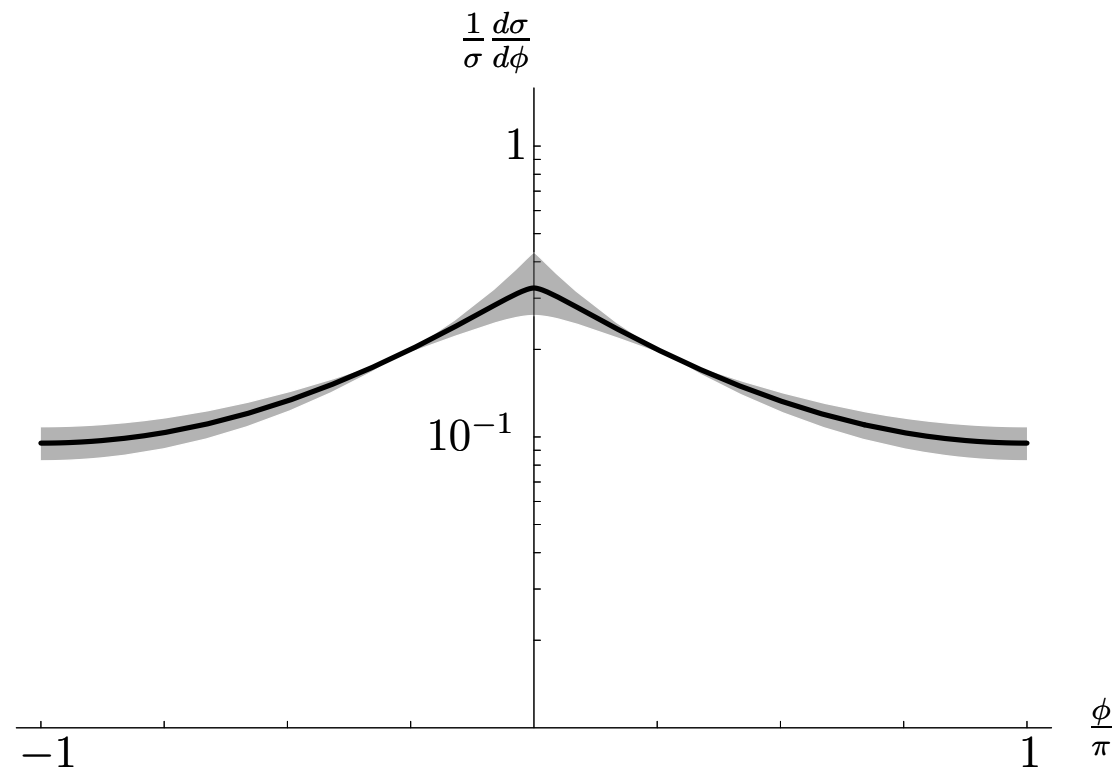
$\frac{1}{N} \frac{dN}{d\phi}$ in a $p\bar{p}$ collider at $\sqrt{s}=1.8$ TeV using a LO (stars), NLO (squares) and resummed (triangles) BFKL kernel. This plot is for $Y = 5$.

5. Azimuthal angles in Mueller–Navelet jets



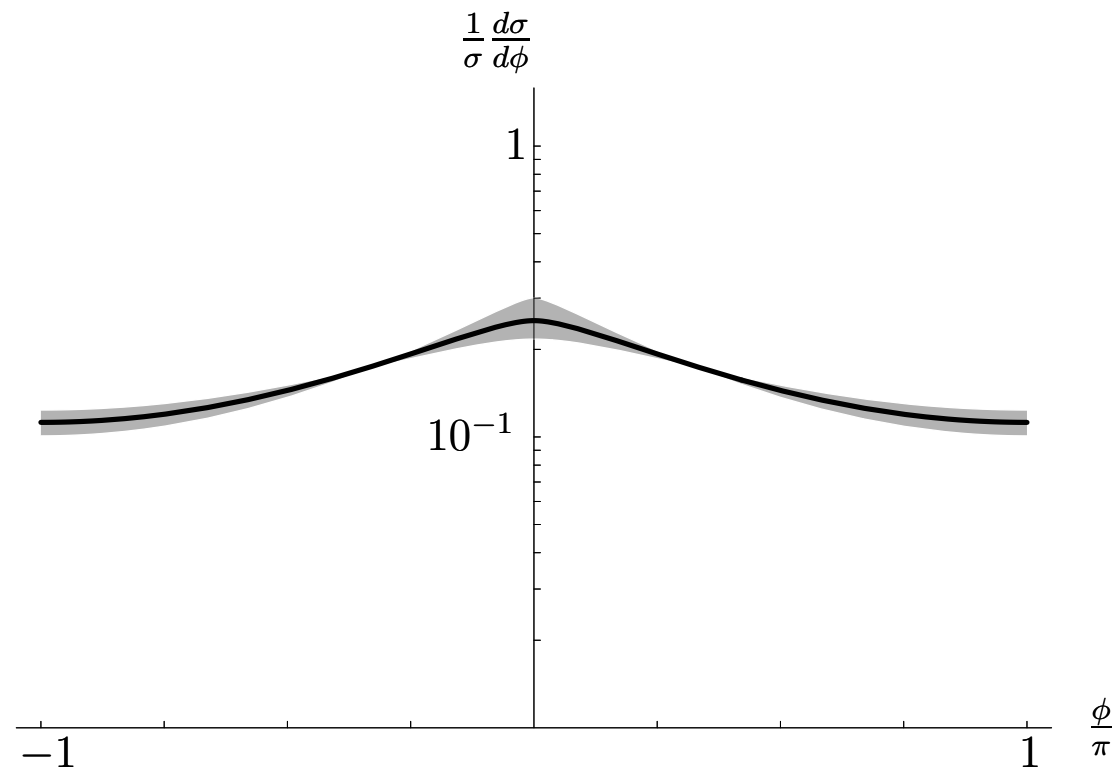
Different ratios of the coefficients \mathcal{C}_n obtained using a collinearly resummed BFKL kernel. The gray band reflects the uncertainty in s_0 and in the renormalization scale μ .

5. Azimuthal angles in Mueller–Navelet jets



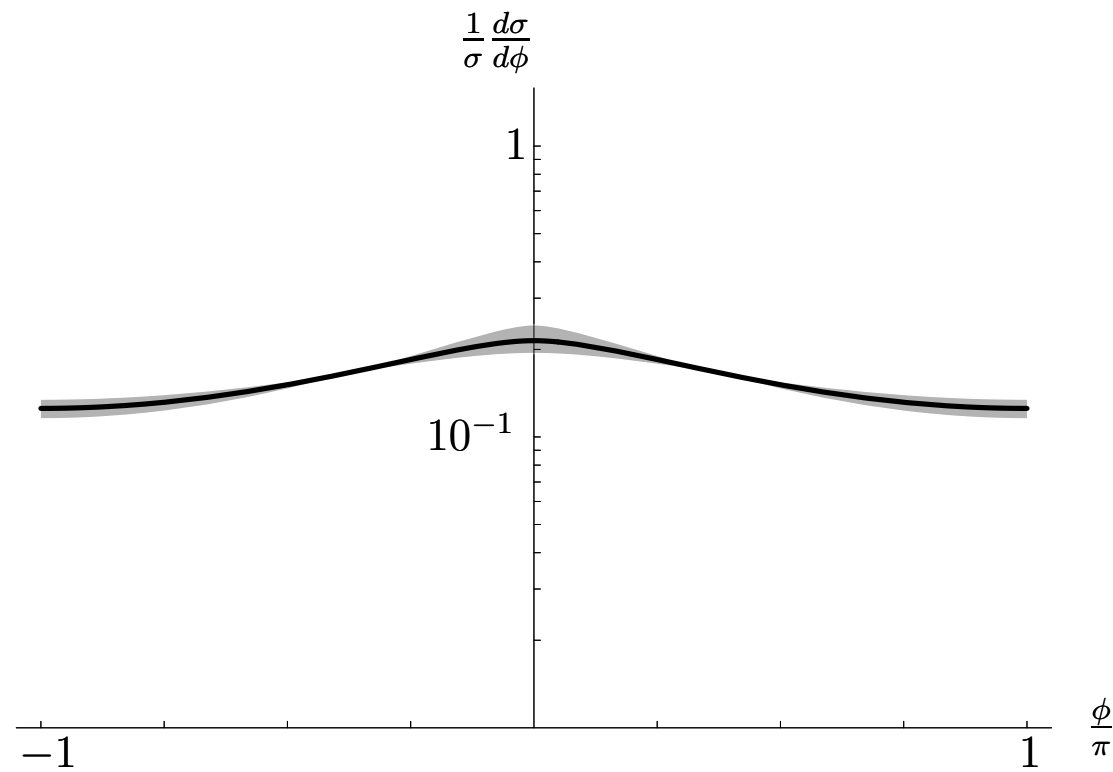
$\frac{1}{\sigma} \frac{d\sigma}{d\phi}$ for $Y = 7$. The gray band reflects the uncertainty in s_0 and in the renormalization scale μ .

5. Azimuthal angles in Mueller–Navelet jets



$\frac{1}{\sigma} \frac{d\sigma}{d\phi}$ for $Y = 9$. The gray band reflects the uncertainty in s_0 and in the renormalization scale μ .

5. Azimuthal angles in Mueller–Navelet jets



$\frac{1}{\sigma} \frac{d\sigma}{d\phi}$ for $Y = 11$. The gray band reflects the uncertainty in s_0 and in the renormalization scale μ .